

HIGHLIGHTS

- We investigate a thick, bioturbated, storm-influenced shallow-marine succession
- We compare several other examples develop in different basin styles
- We challenge that deposition is controlled by frequency and magnitude of storms
- We propose long-term biogenic reworking efficiency is related to basin-scale depositional factors

1
2
3
4
5
6
7
8
9
10
11
12
13
14
15
16
17
18
19
20
21

PALAEO-D-20-00341- Revised version2

Architecture and controls of thick, intensely bioturbated, storm-influenced shallow-marine successions: an example from the Jurassic Neuquén Basin (Argentina)

Schwarz, E.^{1*}, Poyatos-Moré, M.², Boya, S.³, Gomis-Cartesio, L.⁴ and Midtkandal, I.²

1- Centro de Investigaciones Geológicas, Universidad Nacional de La Plata-CONICET, Argentina

2- Department of Geosciences, University of Oslo, Norway

3- Departament de Geologia, Universitat Autònoma de Barcelona, Spain

4- Equinor ASA, Research Centre, Bergen, Norway

*Schwarz, E. Corresponding author. Email: eschwarz@cig.museo.unlp.edu.ar

Poyatos-Moré, M. Email: miquel.poyatos-more@geo.uio.no

Boya, S.: salvaboya@gmail.com

Gomis-Cartesio, L.: LUZG@equinor.com

Midtkandal, I.: ivar.midtkandal@geo.uio.no

Original version: Words: about 5800; 11 Figures, 2 Tables.

Revised version; Words: about 6400; 11 Figures, 2 Tables.

Running title: Thick intensely bioturbated storm-influenced successions

22 **ABSTRACT**

23 Thick (>100 m-thick), highly bioturbated storm-influenced shallow-marine deposits are not
24 frequent in the stratigraphic record, but they tend to be common in aggradational to
25 retrogradational successions. Individual storm-event beds have typically low preservation potential
26 in these successions, yet depositional settings are characterized on the basis of storms processes.
27 Here we present a sedimentological study of a thick, bioturbated exhumed succession deposited
28 during the early post-rift stage of the Neuquén Basin (Argentina) and compare its stratigraphic
29 record with examples worldwide, in order to discuss the potential factors controlling the total
30 overprint of storm-event beds during several million years.

31 The Bardas Blancas Formation being 170-220 m thick in the study area is dominated by muddy
32 sandstones and sandy mudstones, and it also includes subordinate proportions of clean sandstones
33 and pure mudstones, collectively representing different environments of a storm-influenced
34 shoreface-offshore system. The offshore transition and proximal offshore strata invariably comprise
35 intensely bioturbated deposits, with only a few preserved HCS-sandstone beds. The unit shows for
36 most of its thickness a long-term aggradational pattern spanning 7-10 Myr and is associated with
37 low riverine influence.

38 By combining the observations and interpretations of the Bardas Blancas Formation with
39 other subsurface and exhumed intensely bioturbated, shallow-marine successions, we dispute the
40 general assumption that these are associated with low frequency or low magnitude of storms.
41 Alternatively, we argue that the long-lived efficiency of benthic fauna on overprinting most if not all
42 the storm-event beds that reached the offshore-transition sector, results from the combination of
43 several factors: deposition in relatively confined marine depocentres, persistent low riverine
44 influence, and long-term aggradational stacking pattern. As these conditions can develop in a variety
45 of basin styles, such as rift, early post-rift, and foreland settings, the recognition of thick, bioturbated
46 successions as the ones discussed here can be used to infer more realistic constrains for depositional
47 models and better predict facies distribution in such storm-influenced systems.

48

49 *Key words: storm-surge flows, biogenic destruction, long-term aggradational stacking pattern,*
50 *Bardas Blancas Formation.*

51

52

53 **1. Introduction**

54 The deposition and preservation of individual storm-related event beds in shallow-marine
55 settings have been reported and extensively discussed in the literature (Niedoroda et al., 1989;
56 Wheatcroft, 1990; Snedden and Nummedal, 1991; MacEachern and Pemberton 1992; among many
57 others). Facies models for wave- and storm-dominated shoreline and shallow-marine systems are
58 relatively well established (e.g., Walker and Plint, 1992; Reading and Collinson, 1996; Johnson and
59 Baldwin, 1996; Clifton, 2006; Plint, 2010), and they are recently incorporating two-dimensional,
60 quantitative studies for refining shoreline reconstructions (e.g., Isla et al., 2020a, b). MacEachern
61 and Pemberton (1992) characterized three types of shorefaces based on the intensity and frequency
62 of storms: intense, moderate, and weak (low-energy) shorefaces. It is typically assumed that a
63 thoroughly bioturbated succession with little or not preserved storm-event beds within a storm-
64 influenced shoreface-offshore system would represent weakly storm-affected shorefaces
65 dominated by fair-weather deposits (MacEachern and Pemberton 1992; MacEachern et al., 1999,
66 Pemberton et al., 2012).

67 More than 100 m thick successions of storm-influenced, shallow-marine deposits
68 characterized by highly bioturbated strata are not frequent in the stratigraphic record. However,
69 they tend to be unusually common in rift to early post-rift stages of the North Sea Central Graben
70 (Fraser et al., 2003; Gowland, 1996; Howell et al., 1996; Baniak et al., 2014), in rift stages of the
71 North Sea Viking Graben (Råvnas et al., 1997; Løseth et al., 2009), and in early post-rift stages of the
72 South American Neuquén Basin (Bardas Blancas Formation, Veiga et al., 2013). Other unusual
73 examples of highly bioturbated, storm-influenced successions include the Bridport Sand Formation
74 in the extensional Wessex Basin (Morris et al., 2006) and the Late Cretaceous Emery Sandstone
75 Member of the Mancos Shale in the Western Interior foreland basin (Edwards et al., 2005).
76 However, a thorough analysis of all these examples to test if they can be simply placed in the low-
77 energy shoreface end-member of the MacEachern and Pemberton (1992) spectrum, or if there are
78 other controlling factors that contribute to produce thick bioturbated storm-influenced successions,
79 has not yet been attempted.

80 In this study, we present a detailed sedimentological study of a thick, highly bioturbated
81 succession exposed in the northern Neuquén Basin (Lower-Middle Jurassic, Bardas Blancas
82 Formation) with the following objectives: a) to describe and analyse an intensely bioturbated,

83 storm-influenced shallow-marine succession, b) to compare the stratigraphic record of the Bardas
84 Blancas Formation with thick, highly bioturbated units from other basins, c) to discuss the
85 combination of several depositional controls that contribute to the complete destruction of original
86 sedimentary structures and storm-event beds during several million years.

87

88 **2. Geologic and stratigraphic setting**

89 The Neuquén Basin is located on the eastern side of the Andes in west-central Argentina,
90 between latitudes 32° and 40° South, covering an area of over 150,000 km² (Fig. 1A). It comprises a
91 nearly continuous stratigraphic record of up to 6,000 m thick strata from the Upper Triassic to Lower
92 Cenozoic, and it is one of the most important petroleum provinces of South America (e.g. Uliana
93 and Legarreta, 1993). The sedimentary record of the Neuquén Basin includes continental and
94 marine siliciclastics, carbonates, and evaporites, deposited under a variety of basin settings
95 (Legarreta and Uliana, 1991; Howell et al., 2005).

96 During the Late Triassic to Early Jurassic, the western border of Gondwana was characterized
97 by large transcurrent fault systems. This led to extensional tectonics within the Neuquén Basin and
98 the formation of a series of narrow, relatively isolated depocentres (Franzese and Spalletti, 2001),
99 which were filled mostly with volcanic and continental successions (Franzese et al., 2006; D'Elía et
100 al., 2015). Due to continuous subduction at the proto-Pacific margin of Gondwana, a transition from
101 syn- to post-rift conditions occurred in the late Early Jurassic (Vergani et al., 1995), marked by the
102 first marine incursion into the basin (Gulisano et al., 1981; Veiga et al., 2013). The Neuquén Basin
103 became a depocentre with regional slow subsidence in a back-arc position during the sag/post-rift
104 phase that lasted to the end of the Early Cretaceous (Legarreta and Uliana, 1991). In the earliest
105 stage of the post-rift phase, sediment gravity flows and mass movements were particularly common
106 in marine settings, and this has been related to steep gradients (e.g., Legarreta and Uliana, 1996;
107 Burgess et al., 2000; Privat et al., 2020). In this context, low-amplitude eustatic fluctuations, as well
108 as short-lived events of tectonic inversion, probably had a strong influence during the entire post-
109 rift evolution (Legarreta and Uliana, 1991; Howell et al., 2005), but inherited topography and
110 differential compaction had been invoked as potential local factors in the development of early post-
111 rift strata, particularly in the central Neuquén Basin (Cristallini et al., 2009; Veiga et al., 2013).

112 The Cuyo Group represents the early post-rift sedimentation all across the Neuquén Basin
113 (Figs. 1, 2). It commonly overlies the Precuyano volcanic and volcanoclastic succession deposited
114 during the syn-rift stage (Gulisano et al., 1984), but it can also rest directly upon Paleozoic volcanic
115 or plutonic rocks (e.g., Choiyoi Group, Fig. 2). The Cuyo Group spans from Lower to Middle Jurassic
116 and comprises deep-marine to continental deposits in different proportion depending on the
117 position in the basin, with a general east (proximal)-west (distal) depositional trend (Gulisano et al.,
118 1984; Arregui et al., 2011; Brinkworth et al., 2018). In the west-central sector of the Neuquén Basin
119 (Fig. 1), the succession represents continuing deep-water sedimentation, strongly influenced by
120 sediment gravity flows and mass-transport processes (Burgess et al. 2000, Hodgson et al., 2018),
121 and is collectively known as the Los Molles Formation (Gulisano and Gutiérrez Pleimling, 1994). In
122 the study area, in the east-central sector of the basin (Fig. 1A), early post-rift sediments deposited
123 mostly in shallow-marine settings (Veiga et al., 2013), and accumulation started in the Late
124 Toarcian–Aalenian (Riccardi 2008; Spalletti et al., 2012). Lithostratigraphically, in this region the
125 Cuyo Group includes the Bardas Blancas, Los Molles and Lajas formations (Gulisano and Gutiérrez
126 Pleimling, 1994; Spalletti et al., 2012; Veiga et al., 2013) (Fig. 2). The Cuyo Group is truncated by the
127 Intra-Calloviaun unconformity and is overlain by the Lotena Group (Gulisano et al., 1984) (Fig. 2).

128 The Bardas Blancas Formation, the focus of this contribution, is broadly defined as a Lower-
129 Middle Jurassic marine succession (Gulisano and Gutiérrez Pleimling, 1994). It crops out in the
130 Malargüe anticline, particularly in the Potimalal area (Fig. 1A), where it has been described as mostly
131 composed of shoreface to offshore sandstones and mudstones, with subordinated deltaic and
132 terrestrial deposits (Bressan et al., 2013). This unit has been also the focus of investigation in the
133 study area (Sierra de Reyes anticline, Fig. 1A), as part of larger-scale studies including the Cuyo and
134 Lotena Groups (Veiga et al., 2011; Spalletti et al., 2012; Veiga et al., 2013).

135

136 **3. Study area and previous work**

137 Veiga et al. (2013) provided a detailed architectural and sequence stratigraphic analysis of the
138 Bardas Blancas Formation in the Sierra de Reyes study area, integrating outcrop and subsurface
139 information from a 3,000 km² large area. They included two outcrop sections in the western and
140 eastern sectors of the Sierra de Reyes anticline and several wells in the eastern subsurface region
141 (Fig. 2). That study provides a framework in which to place the detailed sedimentological and

142 ichnological analysis of the western outcrops of the Bardas Blancas Formation in the Sierra de Reyes
143 anticline (Fig. 3A).

144 The Sierra de Reyes anticline is located in the southernmost sector of the Malargüe fold and
145 thrust belt, which is the product of tectonic inversion during Late Cretaceous-Neogene times
146 (Giambiagi et al., 2009). The inversion in this region is related to reactivation of Mesozoic normal
147 faults and new reverse structures that transferred shortening to the east (Giambiagi et al., 2009;
148 Sagripanti et al., 2014). The study area in the western flank of the Sierra de Reyes anticline is about
149 5 by 1.5 km, and the strata are mostly dipping 20-30° to the east. The Bardas Blancas Formation is
150 exposed through a series of west-east gullies in which the main sedimentary sections were
151 measured (Fig. 3B). A few reverse faults affect the strata but for the most part the outcrop is laterally
152 continuous and allows reconstruction by means of key stratigraphic markers.

153 The Bardas Blancas Formation is dominated by muddy sandstones and sandy mudstones, and
154 it also includes subordinate proportions of coarser deposits up to pebbly sandstones and pure
155 mudstones. The unit is 170-220 m thick and it unconformably overlies the syn-rift volcanoclastic
156 deposits of the Remoredo Formation across all the area (Figs. 3B, 4A). In the southern sector of the
157 study area (Agua del Ñaco and Agua de Heredia sections, Fig. 3), the Bardas Blancas Formation
158 rapidly grades into a muddy, organic-rich unit defined as part of Los Molles Formation (Gulisano and
159 Gutiérrez Pleimling, 1994; Spalletti et al., 2012) (Fig. 4B, C). The thickness of the Los Molles reaches
160 20 m in the Agua del Ñaco section, and it thins and pinches out to the north. In the Agua del Campo
161 section, the Bardas Blancas strata are sharply overlain by bioclastic and pebbly sandstones of the La
162 Estrechura Member of the Lotena Formation (Veiga et al., 2011; Veiga et al., 2013). Biostratigraphic
163 data based on ammonites of the study succession indicates that the Bardas Blancas Formation in
164 the study area spans from the Late Toarcian to the Early Bathonian (Spalletti et al., 2012) (Fig. 2).
165 According to present chronostratigraphic ages this time span represents no less than 7 Myr and as
166 much as 10 Myr (Cohen et al., 2013). Further to the west of the study area, time-equivalent deposits
167 of the Bardas Blancas Formation are dominantly composed of mudstone strata of the Los Molles
168 Formation, but they occur mostly in the subsurface (e.g., well BjDC.x-1 in Fig. 2).

169 The sequence architecture of the Cuyo Group in this region was investigated by Veiga et al.
170 (2013). Integrating outcrop and subsurface data they identified four parasequence (PS) sets within
171 the study interval (Figs. 2, 4), individually representing alternating conditions from retrogradational
172 (PS Sets I and III) to aggradational (PS Set II), to progradational (PS Set IV) stacking patterns (Fig. 2).

173 Collectively, the lower three parasequence sets were interpreted as representing long-term
174 transgressive conditions during the early post-rift stage of the basin, where sustained
175 accommodation was probably provided by a combination of thermal subsidence, differential
176 compaction of syn-rift deposits and eustatic rise (Veiga et al., 2013). The observed changes in the
177 stacking patterns were attributed to the effect of inherited topography from the underfilled syn-rift
178 half-grabens, as sedimentation areas were expanding during progressive flooding and sediments
179 were depositing in partially filled half-graben-segments with different gradients.

180 For the present study, the sedimentology and stratigraphy of the Bardas Blancas Formation
181 and its transition to Los Molles Formation in the eastern sector of the Sierra de Reyes anticline was
182 recorded by detailed logging of two main sections, namely the Agua de Heredia section
183 (36°55'22.82"S, 69°39'53.77"W), and the Agua del Ñaco section (36°57'9.07"S, 69°40'42.80"W)
184 (Figs. 3B, 4), and complemented with information extracted from the Agua del Campo section of
185 Veiga et al. (2013) (36°54'45.48"S, 69°39'29.94"W). Sedimentological data were recorded in each
186 section (texture, sedimentary structures, palaeocurrents), along with ichnologic, macrofaunal and
187 taphonomic information. Bioturbation intensity was characterized using the Bioturbation Index (BI
188 0-6, Taylor and Goldring, 1993). Sand-silt-mud content in bioturbated facies was visually estimated
189 by using X10 lenses.

190

191 **4. Facies associations and depositional model**

192 The facies and facies associations of the Bardas Blancas Formation and its transition to Los
193 Molles Formation are presented in Table 1. Six facies associations (FA) have been defined for the
194 study interval including: FA1 - Delta front, FA2 - Upper shoreface, FA3 - Lower shoreface, FA4 -
195 Offshore transition, FA5 - Proximal offshore, and FA6 - Distal offshore. The definition and
196 interpretation of these facies associations is broadly in agreement with the proposed by Veiga et al.
197 (2013). Hereby we present a short description of facies associations and their interpretation and
198 subsequently we describe the inferred depositional model.

199

200 **4.1. Delta front (FA1)**

201 FA1 occurs only at the base of the unit and is dominated by pebbly sandstones with planar
202 cross-stratification or horizontal lamination, interbedded with subordinate conglomerates with
203 quartz and volcanic pebbles (up to 5 cm in size), mudstone rip-up clasts and bioclasts in a chaotic to
204 organized fabric (Table 1, Fig. 5A). Poorly defined coarsening-upward successions are observed
205 locally. This association is interpreted to represent a high-energy nearshore setting, heavily
206 influenced by coarse terrestrial input of river-related hyperpycnal flows, and partly reworked by
207 subordinate coastal- wave processes (Veiga et al., 2013).

208

209 **4.2. Upper shoreface (FA2)**

210 FA2 is composed of amalgamated fine- to medium-grained sandstones mostly with trough
211 cross-stratification and occasional lenses of highly fragmented bioclasts (Fig. 5B). Bioturbational
212 structures are absent to low with sparse *Ophiomorpha* (Table 1). This association is thought to
213 reflect a wave-dominated, upper-shoreface setting, intensely affected by longshore currents
214 (Walker and Plint, 1992; Clifton, 2006; Isla et al., 2020a).

215

216 **4.3. Lower shoreface (FA3)**

217 FA3 mostly comprises tabular very fine- to fine-grained sandstones with HCS, and
218 subordinated SCS, plane bed, and symmetrical ripples (Fig. 5C). Bioturbation intensity ranges
219 significantly (BI 2-5) and is dominated by the *Skolithos* ichnofacies (Table 1). This association is
220 interpreted as a lower-shoreface setting dominated by deposits related to storm-surge, purely
221 oscillatory or combined flows (Walker and Plint, 1992, Dumas and Arnott, 2006) with high re-
222 mobilization potential and accordingly, low preservation of fair-weather sediments.

223

224 **4.4. Offshore transition (FA4)**

225 FA4 consists of tabular and massive muddy sandstones and subordinated sandy mudstones
226 (Fig. 5D). Muddy sandstones have up to 30% mud and terrigenous coarse silt and very fine sands
227 dominate, whereas in sandy mudstones the mud fraction is estimated in about 50 to 70%.
228 Bioturbation was mostly intense (BI 5-6), locally moderate (BI 4). A highly diverse *Cruziana*
229 ichnofacies dominates (Table 1) in which *Teichichnus* and *Chondrites* prevail (Fig. 6A, B).

230 Infrequently, medium- to thin-bedded, very-fine grained sandstones with HCS are recorded in this
231 association. These beds invariably show an increment of bioturbation intensity at the top, passing
232 abruptly to completely bioturbated muddy sandstones. This association is inferred to represent an
233 offshore-transition setting, immediately below the fair-weather wave-base (Reading and Collinson,
234 1996; Schwarz et al., 2013). Storm-surge flows delivered sand to distal marine settings, but post-
235 depositional bioturbation mixed mud and sandy event beds into muddy sandstones in almost all
236 cases.

237

238 **4.5. Proximal offshore (FA5)**

239 FA5 is dominated by massive sandy and silty mudstones forming tabular beds with diffuse
240 bedding planes (Fig. 5E). Bioturbation intensity is systematically high (BI 5-6). Ichnologically, a distal
241 expression of the *Cruziana* ichnofacies is encountered (Table 1). *Chondrites*, *Rhizocorallium*, and
242 *Zoophycos* sporadically occur in outcrops (Fig. 6C, D), whereas smaller traces such as *Phycosiphon*
243 or *Helminthopsis* are commonly observed in cores of these sandy and silty mudstones (Veiga et al.,
244 2013, their figure 9c). As in FA4, very uncommon discrete sandstone beds occur interbedded in this
245 association, but they tend to be finer grained and thinner than the ones interbedded in that facies
246 association (Table 1). Due to the relatively lower proportion of sand in this association than in FA4,
247 FA5 is interpreted as a proximal-offshore setting, representing the distal end of the running-distance
248 of most storm-derived flows (Veiga et al., 2013).

249

250 **4.6. Distal offshore (FA6)**

251 FA6 includes mudstone-dominated successions that are common at the base and top of the
252 study interval (Fig. 2, 5F). At the base, they consist of grey, massive, moderately bioturbated
253 mudstones, grouped into the *Zoophycos* ichnofacies (Table 1) that is commonly observed in cores
254 (Veiga et al., 2013, their figure 9D). Medium- to thin-bedded conglomerate layers with
255 extraformational pebbles and mudstone rip-up clasts are locally interbedded in these mudstone
256 beds. At the top of the unit, towards the Los Molles Formation, FA6 is mostly represented by black,
257 fissile (platy), unbioturbated shales in which cm-thick tuffaceous layers occur. FA6 is interpreted to
258 reflect the distal conditions of an offshore to shelf setting, but under two different conditions: the
259 oxic sea-floor conditions as well as sediment gravity flows depositing coarse material were common

260 when the distal offshore deposits of the early Bardas Blancas Formation accumulated; the overlying
261 Los Molles Formation, however, exhibit high organic contents and original lamination that points to
262 long-lived dysoxic to anoxic conditions (Doyle et al. 2005, Veiga et al., 2013).

263

264 **4.7. Depositional model**

265 Except for FA1 that is solely recorded at the base of the Bardas Blancas Formation (Table 1),
266 the remaining facies associations are commonly stacked to form up to a few tens of meters thick
267 shallowing-upward successions. Thus, a well-defined storm- and wave-dominated shoreface-
268 offshore depositional system is reconstructed for the unit (Fig. 7). The upper-shoreface was
269 dominated by migrating dunes and bars associated with long-shore currents (FA2), whereas the
270 adjacent lower-shoreface setting mostly exhibits event beds with HCS formed by the development
271 of storm-surge combined flows (FA3, Fig. 7). The bioturbation intensity within the shoreface
272 deposits increases offshore and hence, follows the normal pattern for wave-dominated shoreface-
273 offshore systems (Reineck and Howard, 1981; Walker and Plint, 1992; Gowland, 1996; Hampson,
274 2000; MacEachern et al., 2007; Schwarz et al., 2016, 2018).

275 In marked contrast, the preservation motifs and inferred conditions in the offshore transition
276 (FA4) and proximal offshore (FA5) appear quite peculiar. These two adjacent settings record
277 depositional conditions between fair-weather and storm wave-base (Fig. 7), and show a gradual
278 increase in the proportion of mud versus sand fraction, because the storm-surge flows could export
279 decreasing amounts of sand to more distal areas (Aigner and Reineck, 1982; Plint, 2010). With
280 respect to the post-depositional mixing of mud and sand, these two environments are very similar,
281 providing a similar capacity of burrowing organisms to rework almost 100% of the sands between
282 the events. The fact that these conditions prevailed for a long period of time (7 to 10 Myr) is not a
283 commonly reported motif for examples worldwide and is further discussed in this contribution.

284 In the distalmost segment of the interpreted shoreface-offshore system, accumulation of
285 mud prevailed and is considered to have been accumulated dominantly from settling out of
286 suspensions in very low-energy hydrodynamic settings (FA6). Debris flows transporting gravel were
287 common in early stages of the system (Fig. 7), but probably became infrequent later in its evolution,
288 allowing to produce a mud-rich, distal offshore, occasionally colonized by *Zoophycos*-producing
289 organisms. Distal offshore settings prevailed further to the west of the study area were substrate

290 conditions probably remained constant during most of the Bardas Blancas Formation deposition
291 (Figs. 2, 7). When a distal offshore setting was established in the southern sector of the study area
292 (Los Molles Formation), a shift to prevailing dysoxic-anoxic conditions appears to have dominated
293 in the sea-floor.

294

295 **5. Architecture of an intensely bioturbated succession**

296 The shallowing-upward units identified in the Bardas Blancas are parasequences bounded by
297 flooding surfaces (Figs. 4, 8A), uncommonly demarcated by shell beds. These stratigraphic units are
298 internally composed of bedsets with subtle stratigraphic boundaries (Fig. 8A). In the lower interval
299 of the unit, parasequences show a complete transition from mudstones of FA6 (distal offshore) to
300 clean, trough cross-bedded sandstones of FA2 (upper shoreface) (Fig. 4). In the middle and upper
301 intervals of the Bardas Blancas Formation, parasequences are mostly composed of sandy mudstones
302 and muddy sandstones of FA5 and FA4 (proximal offshore and offshore transition), sometimes with
303 the presence of lower-shoreface HCS-sandstones at their top (FA4) (Figs. 8A). Bioturbation intensity
304 in the lower-shoreface deposits is either similar or lower than the one recorded in the underlying
305 offshore-transition facies (Fig. 8A).

306 The most distinctive feature of the Bardas Blancas Formation is that most of the proximal
307 offshore (FA5) and offshore transition (FA4) strata are intensely bioturbated (BI 5-6). Complete
308 bioturbation (BI 6) is dominant and results in a completely structureless appearance of the beds (Fig.
309 8B, Taylor and Goldring, 1993; Wetzel and Uchmann, 1998). It also typically prevents the
310 identification of individual trace fossils. In these two facies associations, beds are defined by subtle
311 variation in the sand-silt-mud content, usually aided by the weathering profile, where the muddier
312 facies is less resistant (Fig. 8B). The relative dominance of muddy sandstones versus sandy and silty
313 mudstones in a given interval defines the presence of FA4 or FA5 (Fig. 8B, C). Individual beds range
314 from 0.10 m up to 1.5 m in thickness and they almost invariably show planar, horizontal lower and
315 upper contacts defining tabular beds at different scales, from a few 10s to 100s of meters in length
316 (Fig. 8C, D).

317 Despite the intense bioturbation, these two facies associations contain sparsely
318 unbioturbated sandstone beds providing information for interpreting their primary depositional
319 processes. Where observed, these sandstone beds commonly have hummocky cross-stratification

320 and are laterally continuous for up to a few 10s of meters (Fig. 9A, D). They have a sharp, irregular
321 base overlying silty mudstone and invariably show an irregular, transitional or sharp top to muddy
322 sandstones (Fig. 9B, E). In these overlying muddy sandstone, bioturbation intensity is moderate to
323 high (BI 4-5), and an ichnofabric dominated by *Chondrites* can be recognized in outcrop (Fig. 9C);
324 however, a more diverse assemblage including *Phycosiphon* and *Zoophycos* has also been recorded
325 in cores of the unit (Veiga et al., 2013). The discrete storm-generated deposit rapidly becomes a
326 completely bioturbated muddy sandstone laterally, and exhibits the typical weathering profile as all
327 of the similar beds (Fig. 9A, D).

328 The aggradational to retrogradational stacking pattern of Parasequence Sets II and III has a
329 major impact in the resulting distinctive stratigraphic architecture of the study succession (Figs. 2,
330 4). As a result of these long-term aggradational conditions, about 100 m of the Bardas Blancas
331 Formation in the study area are dominated by a vertical stacking of almost completely mixed
332 deposits of FA4 and FA5 (Figs. 4, 8 and 9). The resulting stratigraphy is a storm-generated, but highly
333 bioturbated, thick monotonous succession, with very little grain size variation (muddy sandstones
334 to sandy mudstones), virtual absence of preserved primary physical (sedimentary) structures,
335 bedding contacts that are invariably horizontal, and scattered fossil remains that rarely produce
336 distinct shell concentrations.

337

338 **6. Discussion**

339 The preservation potential of individual storm-related event beds (or tempestites) in shallow-
340 marine settings and the lam-scam textures resulting from partial to total biogenic reworking of
341 these event beds have been extensively reported and discussed (Wheatcroft, 1990; MacEachern
342 and Pemberton 1992; among many others). Three types of shoreface settings are distinguished
343 based on the intensity and frequency of storms: intense, moderate, and weak or low-energy
344 (MacEachern and Pemberton, 1992). Commonly is assumed that a thoroughly bioturbated
345 succession with little or no preserved tempestites within a storm-influenced shoreface-offshore
346 system would represent weakly storm-affected shoreface facies dominated by fair-weather
347 deposits. Following this reasoning, stacked, well-preserved tempestites would be interpreted as
348 storm-dominated shoreface deposits (MacEachern and Pemberton 1992; MacEachern et al., 1999,
349 Pemberton et al., 2012).

350 The facies associations interpreted to represent offshore-transition (partially equivalent to
351 the “distal lower shoreface” of MacEachern et al., 1999) to proximal offshore settings of the Bardas
352 Blancas Formation are invariably composed of highly bioturbated muddy sandstones, sandy
353 mudstones, and very few preserved tempestites. Most, if not all, of the presently bioturbated
354 deposits were delivered by storm-surge flows. Following the MacEachern and Pemberton (1992)
355 characterization, the Bardas Blancas system would, therefore, match the low-energy category of the
356 storm-influenced shoreface systems.

357

358 **6.1. Thick bioturbated storm-influenced shallow-marine successions: where do they occur?**

359 Monotonous, more than 100 m thick successions of storm-influenced, shallow-marine
360 deposits formed by persistent combination of processes that resulted in highly bioturbated strata
361 are not common in the stratigraphic record, but they tend to be restricted to certain conditions
362 (Figs. 10, 11; Table 2). The Upper Jurassic Farsund Formation in the Norwegian Central Graben (distal
363 equivalent of the Ula Formation, Bergan et al., 1989; Fraser et al., 2003), the Upper Jurassic Heather
364 and Lower Kimmeridge Clay formations in the UK Central Graben (distal equivalents of the Fulmar
365 Formation, Donovan et al., 1993; Gowland, 1996), and the transition from the Middle Jurassic
366 Tarbert to Heather Formations in the North Viking Graben (Råvnas et al., 1997; Råvnas and Steel,
367 1998; Løseth et al., 2009) are all subsurface examples showing facies and bioturbation patterns that
368 are remarkably similar to the ones observed in outcrops and subsurface for the Bardas Blancas
369 Formation (Fig. 10D). The Lower to Middle Jurassic Bridport Sand Formation in the Wessex Basin
370 (Morris et al., 2006) and the Upper Cretaceous Emery Sandstone Member of the Mancos Shale
371 (Edwards et al., 2005) provide outcrop examples of highly bioturbated shallow-marine successions.

372 The Farsund Formation in the Norwegian Central Graben is dominated by intensely
373 bioturbated muddy sandstones and sandy mudstones reaching 200 m in thickness in Well 2/1-6 (Fig.
374 10A) (FactPages - Norwegian Petroleum Directorate, 2020). The equivalent more proximal Ula
375 Formation is mostly composed of highly bioturbated sandstones, interpreted to reflect weak to
376 moderate shoreface types (Baniak et al., 2014, 2015), following the model from MacEachern and
377 Pemberton (1992). The sedimentology and ichnology of the Fulmar Formation in the UK Central
378 Graben has been described in detail by Howell et al. (1996) and Gowland (1996). They concur on
379 the long-lived development of a storm-influenced shoreface-offshore system, in which intense
380 bioturbation extinguished depositional structures largely in the lower shoreface and offshore-

381 transition settings (Fig. 10B). As in the Ula Formation, intense bioturbation in the offshore transition
382 zone of the Fulmar Formation was interpreted as the result of low magnitude and/or low frequency
383 of storm events (Howell et al., 1996). Collectively, these Upper Jurassic units of the Central Graben
384 developed in a rifting regime and show long-term (several million years) aggradational to
385 retrogradational stacking patterns (Howell et al., 1996; Mannie et al., 2014; 2016) (Fig 11).

386 The facies associations and stacking patterns of the Tarbert and Lower Heather succession in
387 the North Viking Graben were described by Løseth et al. (2009), based on cores and several key
388 wells including well 30/9-14 (Fig. 10C) . In this well, the gamma-ray log for most of the Lower Heather
389 interval shows a very uniform response and cores display relatively homogeneous, highly
390 bioturbated muddy sandstones (Fig. 10C) grading into bioturbated sandstones with poorly
391 preserved HCS beds. This uppermost succession has been interpreted to represent a parasequence
392 with progradation from offshore, into offshore-transition settings and lowermost shoreface, within
393 a long-term retrogradational stacking pattern (Løseth et al., 2009) (W3 in Fig. 11). These authors
394 suggested that bioturbation intensity increases from W2 to W3 within the retrogradational stacking
395 pattern (Løseth et al., 2009, their figure 4). This net transgressive trend developed within a syn-rift
396 setting during the Bathonian and probably lasted for 1-2 Myr (Mannie et al., 2016).

397 The Lower to Middle Jurassic Bridport Sand Formation in the Wessex Basin (UK) is another
398 example of a storm-influenced, intensely bioturbated succession (Morris et al., 2006). According to
399 the high degree of biogenic reworking, the dominant siltstones and silty sandstones with uncommon
400 preserved storm beds were interpreted as reflecting low-energy lower-shoreface and offshore-
401 transition settings (Morris et al., 2006). Interestingly, no evidence of nearby fluvial influence or river-
402 mouth processes were recorded, and sand supply to the shoreface settings was related to along-
403 shore transport. Moreover, the unit was attributed to represent a long-term aggradational stacking
404 pattern developed in an extensional fault-bounded depocentre, formed due to localized high
405 tectonic subsidence (Morris et al., 2006) (Table 2). A well exposed example of thick, highly
406 bioturbated storm-influenced shallow-marine deposits occurs within the Upper Cretaceous Emery
407 Sandstone Member of the Mancos Shale (Book Cliffs, Utah, USA). This units is up to 250 m thick and
408 represents an aggradational stack of storm-dominated shoreface parasequences developed in a
409 foreland basin (Edwards et al., 2005) (Table 2).

410 All of these examples illustrate that the Bardas Blancas Formation is a good analogue for thick
411 bioturbated shallow-marine successions occurring in a variety of basinal settings, but preferentially

412 in those where: (1) storm-surges act as main across-offshore transport within relatively confined or
413 small marine depocentres, (2) the fluvial influence is low to moderate, and (3) on the long-term the
414 sediment supply and accommodation is balanced and expressed by aggradational stacking patterns
415 (Fig 11). Thus, it is an oversimplification to assume that these depositional conditions would be
416 overruled by the frequency and magnitude of atmospheric processes (such as the storms), which
417 also vary significantly during the long-term periods represented by these successions.

418

419 **6.2. Factors fostering thick bioturbated storm-influenced shallow-marine successions**

420 Based on the occurrence of similar, thick, storm-generated, shallow-marine successions
421 sharing more geological attributes than just their highly bioturbated nature, we propose to relate
422 the intense bioturbational mixing of the original storm beds and sedimentary structures over several
423 million years to a suite of factors, rather than constant low frequency and/or magnitude of
424 atmospheric processes (the storms).

425 Most of the examples mentioned above are related to complex syn-rift or early post-rift
426 topography, which defines relative small depocentres during long-term marine transgressions
427 (Howell et al., 1996; Veiga et al., 2013). These depocentres were mostly elongated and a few to tens
428 of kilometers wide (Fig. 11). This depositional context is essential for the benthic fauna to inhabit
429 almost the entire extent of these small depocentres, to produce not only total bioturbation in
430 vertical sections (as seen in 1D cores, Fig. 10), but also to obliterate original beds for several
431 kilometers laterally, as recorded in the outcrops of the Bardas Blancas Formation. In other words,
432 we relate the relatively small size of the depositional setting to the high efficiency of benthic fauna
433 to rework most of the individual storm deposits, independently of how fast the benthos establishes
434 on the event bed, or the storm frequency. This bioturbational mixing efficiency is steadily high across
435 the depositional environment, from the lower shoreface to proximal offshore, and does not
436 necessarily follow the trends observed on modern shelves (Reineck, 1977; Howard and Reineck,
437 1981). Howell et al. (1996) already used this basin-scale factor to support their process-realistic
438 depositional model for the bioturbated, sand-dominated deposits of the Fulmar Formation.
439 Moreover, Morris et al. (2006) suggested that small areas of accumulation in the Bridport Formation
440 could have been more prone to extensive biotic proliferation, increasing the destruction success of
441 storm-event beds. Going further, it can be speculated that relatively small-sized depocentres would

442 allow a more homogeneous distribution of the food source for the benthic fauna, which would
443 ultimately account for its success in utilizing the entire depositional setting at all times.

444 An additional, long-term control on these thick bioturbated successions is related to the
445 potential riverine water, sediment, and solute input to the marine realm. Modern studies have
446 shown that individual, hurricane-related storm-event beds have high probability to be completely
447 destroyed by bioturbation when riverine influence is relatively low and water depth is shallow (< 30
448 m), for example in the inner shelf of the Gulf of Mexico (Snedden and Nummedal, 1991; Dashtgard
449 et al., 2015). Likewise, it has also been recently demonstrated that amalgamated storm beds can be
450 completely bioturbated fairly rapidly (< 10 years) under conditions of high riverine influence, such
451 as several hurricane-event layers described immediately downdrift of the Mississippi River delta, in
452 similar water depths (Walsh et al., 2018).

453 The stratigraphic record of the intensely bioturbated succession reported in our study
454 suggests a sustained biogenic reworking efficiency close to 100% during several million years (Fig.
455 11). Consequently, ecologic factors affecting the benthic fauna typically associated with nearby, high
456 riverine influence, such as turbidity or salinity fluctuations, were short-lived or uncommon episodes
457 in the reported depositional settings. Therefore, for most of the Bardas Blancas Formation (PS Sets
458 II and III, Fig. 4) we infer that riverine entry points were far from the study area and sand was
459 supplied mostly by along-shore transport. This seems to be the case also for other examples
460 discussed in section 6.1 and shown in Table 2. Howell et al. (1996) inferred absence of large deltas
461 and low-discharge fluvial systems to deliver the clastic supply for the marine sandstones of the
462 Fulmar Formation, whereas Morris et al. (2006) related the highly bioturbated succession to the lack
463 of nearby river-mouth processes and significant along-shore transport. Significantly, the intensely
464 bioturbated Emery Member was formed when small rivers drained the Sevier Orogen, rather than
465 a large fluvial system as inferred for the shoreface settings of the underlying and overlying units
466 (Edwards et al., 2005).

467 Another evident similarity between all the aforementioned examples is associated with the
468 long-term stacking pattern (Fig. 11). The early post-rift Bardas Blancas Formation and the rift to early
469 post-rift successions of the Central Graben show a consistent aggradational to retrogradational
470 stacking covering from 7 to 20 Myr (Fig. 11) (Table 2). The transition from the fluvial to estuarine
471 deposits of the Tarbert Formation and thereafter into the marine deposits of the lower Heather
472 Formation, represents at the base a net retrogradational trend that becomes more aggradational-

473 to-retrogradational upward (W2 and W3, Fig 11). Interestingly, the overall bioturbation index in the
474 offshore-transition deposits increases in the W3 interval (Løseth et al., 2009), suggesting that the
475 maximum bioturbational mixing efficiency of storm-event beds occurred at that time.

476 The Emery Sandstone succession represents another unusual record of long-term
477 aggradational stacking pattern (1.7 Myr, Table 2), in which the sedimentation rates were low
478 compared to those of the underlying and overlying units (Edwards et al, 2005). Coincidentally, the
479 offshore-transition to lower-shoreface deposits of the Emery Sandstone reflect one of the highest
480 bioturbational mixing efficiency of storm-event beds in the Upper Cretaceous record of the
481 Wasatch-Book Cliff section (Edwards et al, 2005). This shows a marked difference with less
482 bioturbated, environment-equivalent deposits, for example the younger Kenilworth Member (Eide
483 et al., 2015) and the Grassy Member (Onyeonu et al., 2018) of the Blackhawk Formation, both units
484 developed in progradational stacking patterns. Thus, a delicate long-lived balance between
485 sediment supply and accommodation to create thick successions with highly aggradational (to
486 slightly retrogradational) stacking patterns could be linked to sedimentation rates across the
487 shoreface-offshore system. The offshore-transition and proximal offshore sectors of the system
488 would have experienced low net sedimentation rates that – if all other variables remained fairly
489 constant – would have produced a similar effect than low frequency storm-surge flows reaching
490 those regions. The lack of significant progradational events expressed by basinward facies shifts also
491 contributed to create thick, fairly homogeneous strata, without major breaks in sedimentation or
492 sequence boundaries, and representing only one or two segments of the depositional system. In the
493 case of the investigated examples, those segments correlated approximately with the areas
494 between the fair-weather and the storm wave-base, in which the highest bioturbational mixing
495 efficiency of storm-event beds took place.

496 By combining the observations and interpretations of different thick, intensely bioturbated,
497 shallow-marine successions the common assumption that the final bioturbated product can be
498 associated only to low frequency or magnitude of storm events is questionable. Alternatively, the
499 long-lived efficiency of benthic fauna reworking most if not all the storm-event beds reaching the
500 offshore transition sector, results from the combination of two or three factors: (1) deposition in
501 relatively confined marine depocentres, (2) persistent low fluvial influence, and (3) a long-term,
502 aggradational to slightly retrogradational stacking pattern. As these conditions can be develop in a
503 variety of basin styles, such as rift, early post-rift, and foreland settings, the recognition of thick,

504 bioturbated successions as the ones discussed here can be used to infer more realistic constrains
505 for depositional models and to better predict facies distribution in such storm-influenced systems.

506

507 **7. Conclusions**

508 1 - The Lower-Middle Jurassic Bardas Blancas Formation represents an up to 220 m thick, highly
509 bioturbated, storm-influenced shallow-marine succession developed during the early post-rift
510 stage of the Neuquén Basin.

511 2 - Most of its stratigraphic record is dominated by muddy sandstones and sandy to silty mudstones
512 deposited in offshore-transition to proximal-offshore settings, in which benthic- fauna efficiency
513 to rework individual storm-event beds was persistently close to 100 % during a time span ranging
514 from 7 to 10 Myr. This highly efficient biogenic reworking was mostly associated to deposit-
515 feeding organisms of the *Cruziana* ichnofacies.

516 3 - The Bardas Blancas Formation shares several attributes with other > 100 thick, intensely
517 bioturbated successions including: (i) deposition in relatively confined marine depocentres, (ii)
518 persistent low riverine influence, and (iii) long-term (2 -20 Myr) aggradational stacking pattern.
519 Yet, all these biogenically reworked successions are developed in a variety of structural styles,
520 including rift, early post-rift, and foreland settings.

521 4 – Therefore, it is questionable to assume that the resulting architecture of these unusually thick,
522 bioturbated shoreface-offshore successions at different scales should be directly associated to
523 low-frequency or magnitude storms. Alternatively, the long-lived efficiency of benthic fauna
524 reworking almost all the storm-event beds formed in these depositional environments during
525 several million years was more likely controlled by the co-occurrence of the following
526 depositional factors: a) relatively small depocenters with infauna evenly distributed in
527 intermediate to distal sectors, b) benthic fauna very rarely affected by considerable physico-
528 chemical changes in those regions due to overall low riverine influence, and c) delicate balance
529 between sediment supply and accommodation producing an aggradational stacking and
530 relatively low net sedimentation rates across the depositional area.

531 5 - These depositional conditions can establish in a variety of basin styles, so the outlined factors
532 controlling the formation of thick, highly bioturbated successions can be applied to infer more

533 realistic constrains for depositional models and improving facies predictions in such confined
534 storm-influenced systems.

535

536 **Acknowledgments**

537 E.S. would like to thank CONICET and Universidad Nacional de La Plata for partially supporting this
538 project. M.P. and I.M. acknowledge Aker BP, sponsor of the ShelfSed project (University of Oslo).
539 We thank J. Cuitiño and A. Weztel for their constructive reviews and specifically the latter for his
540 dedicated revision of the English writing. An anonymous reviewer also provided additional
541 comments. We are also grateful to Francisco Rodriguez-Tovar for the invitation to participate in
542 this special publication.

543

544 **References**

545 Aigner, T., Reineck, H.-E., 1982. Proximality trends in modern storm sands from the Helgoland Bight
546 (North Sea) and their implications for basin analysis. *Senckenbergiana Maritima* 14, 183–215.

547 Arregui, C., Carbone, O., Martínez, R., 2011. El Grupo Cuyo (Jurásico Temprano-Medio) en la Cuenca
548 Neuquina, Geología y Recursos Naturales de la Provincia del Neuquén: Buenos Aires, Relatorio del
549 18 Congreso Geológico Argentino, pp. 77-89.

550 Baniak, G.M., Gingras, M.K., Burns, B.A., Pemberton, S.G., 2014. An example of a highly bioturbated,
551 storm-influenced shoreface deposit: Upper Jurassic Ula Formation, Norwegian North Sea.
552 *Sedimentology* 61, 1261-1285.

553 Baniak, G.M., Gingras, M.K., Burns, B.A., Pemberton, S.G., 2015. Petrophysical characterization of
554 bioturbated sandstone reservoir facies in the Upper Jurassic Ula Formation, Norwegian North Sea,
555 Europe. *Journal of Sedimentary Research* 85, 62-81.

556 Bergan, M., Tørudbakken, B., Wandås, B., 1989. Lithostratigraphic correlation of Upper Jurassic
557 sandstones within the Norwegian Central Graben: sedimentological and tectonic implications, in:
558 Collinson, J.D. (Ed.), *Correlation in Hydrocarbon Exploration*. Springer Netherlands, Dordrecht, pp.
559 243-251.

560 Bressan, G.S., Kietzmann, D.A., Palma, R.M., 2013. Facies analysis of a Toarcian/Bajocian shallow
561 marine/coastal succession (Bardas Blancas Formation) in northern Neuquén Basin, Mendoza
562 province, Argentina. *Journal of South American Earth Sciences* 43, 112-126.

563 Brinkworth, W., Vocaturo, G., Loss, L., Giunta, D., Mortaloni, E., and Massaferro, J.L., 2018. Estudio
564 cronoestratigráfico y evolución paleoambiental del Jurásico Inferior-Medio en el Engolfamiento de
565 la Cuenca Neuquina, Argentina, in Gardini, M., Gómez, M., Manceda, R., Ayoroa, M.A., Limeres, M.,

- 566 Peroni, G., Cruz, C.E., Malone, P., and Villar, H. (Eds.), Sesiones Generales, 10º Congreso de
567 Exploración y Desarrollo de Hidrocarburos, Mendoza, Argentina: Instituto Argentino del Petróleo,
568 pp. 597-621.
- 569 Burgess, P.M., Flint, S., Johnson, S., 2000. Sequence stratigraphic interpretation of turbiditic strata:
570 An example from Jurassic strata of the Neuquén basin, Argentina. *GSA Bulletin* 112, 1650-1666.
- 571 Clifton, H.E., 2006. A re-examination of facies models for clastic shorelines, in Posamentier, H.W.,
572 and Walker, R.G. (Eds.), *Facies Models Revisited*. Society for Sedimentary Geology, Special
573 Publications, 84, pp. 293–337.
- 574 Cohen, K.M., Finney, S.C., Gibbard, P.L., Fan, J.-X. (2013; updated). The ICS International
575 Chronostratigraphic Chart. Episodes 36: 199-204. V2020/03. WWW.stratigraphy.org
- 576 Dashtgard, S.E., Snedden, J.W., MacEachern, J.A., 2015. Unbioturbated sediments on a muddy shelf:
577 Hypoxia or simply reduced oxygen saturation?. *Palaeogeography, Palaeoclimatology,*
578 *Palaeoecology*, 425, 128-138.
- 579 D'Elia, L., Bilmes, A., Franzese, J.R., Veiga, G.D., Hernández, M., Muravchik, M., 2015. Early evolution
580 of the southern margin of the Neuquén Basin, Argentina: Tectono-stratigraphic implications for rift
581 evolution and exploration of hydrocarbon plays. *Journal of South American Earth Sciences* 64, 42-
582 57.
- 583 Donovan, A.D., Djacic, A.W., Ioannides, N.S., Garfield, T.R., Jones, C.R., 1993. Sequence stratigraphic
584 control on Middle and Upper Jurassic reservoir distribution within the UK Central North Sea.
585 Geological Society, London, Petroleum Geology Conference series 4, 251-269.
- 586 Doyle, P., Poiré, D.G., Spalletti, L.A., Pirrie, D., Brenchley, P., Matheos, S.D., 2005. Relative
587 oxygenation of the Tithonian — Valanginian Vaca Muerta—Chachao formations of the Mendoza
588 Shelf, Neuquén Basin, Argentina, in: Veiga, G., Spalletti, L., Howell, J., Schwarz, E. (Eds.), *The*
589 *Neuquén Basin: A Case Study in Sequence Stratigraphy and Basin Dynamics*. Geological Society,
590 London, Special Publications, 252, pp. 185-206.
- 591 Dumas, S., Arnott, R.W.C., 2006. Origin of hummocky and swaley cross-stratification— The
592 controlling influence of unidirectional current strength and aggradation rate. *Geology* 34, 1073-
593 1076.
- 594 Edwards, C.M., Howell, J.A., Flint, S.S., 2005. Depositional and stratigraphic architecture of the
595 Santonian Emery Sandstone of the Mancos Shale: Implications for Late Cretaceous evolution of the
596 Western Interior foreland basin of Central Utah, U.S.A. *Journal of Sedimentary Research* 75, 280-
597 299.
- 598 Eide, C.H., Howell, J.A., Buckley, S.J., 2015. Sedimentology and reservoir properties of tabular and
599 erosive offshore transition deposits in wave-dominated, shallow-marine strata: Book Cliffs, USA.
600 *Petroleum Geoscience* 21, 55-73.
- 601 FactPages - Norwegian Petroleum Directorate (2020), <http://factpages.npd.no/factpages/>.

- 602 Franzese, J.R., Spalletti, L.A., 2001. Late Triassic–early Jurassic continental extension in
603 southwestern Gondwana: tectonic segmentation and pre-break-up rifting. *Journal of South*
604 *American Earth Sciences* 14, 257-270.
- 605 Franzese, J.R., Veiga, G.D., Schwarz, E., Gómez-Pérez, I., 2006. Tectonostratigraphic evolution of a
606 Mesozoic graben border system: the Chachil depocentre, southern Neuquén Basin, Argentina.
607 *Journal of the Geological Society* 163, 707-721.
- 608 Fraser, S.I., Robinson, A.M., Johnson, H.D., Underhill, J.R., Kadolsky, D.G.A., Connell, R., Johannesen,
609 P., Ravnås, R., 2003. Upper Jurassic, in: Evans, D., Graham, C., Armour, A., Bathurst, P. (Eds.), *The*
610 *Millennium Atlas: Petroleum Geology of the Central and Northern North Sea*. The Geological Society
611 of London, London, UK, pp. 157-189.
- 612 Giambiagi, L., Tunik, M., Barredo, S., Bechis, F., Ghiglione, M., Alvarez, P., Drosina, M., 2009.
613 Cinemática de apertura del sector norte de la cuenca Neuquina. *Revista de la Asociación Geológica*
614 *Argentina* 65, 278-292.
- 615 Gowland, S., 1996. Facies characteristics and depositional models of highly bioturbated shallow
616 marine siliciclastic strata: an example from the Fulmar Formation (Late Jurassic), UK Central Graben.
617 *Geological Society, London, Special Publications* 114, 185-214.
- 618 Gulisano, C.A., 1981. El Ciclo Cuyano en el norte de Neuquén y sur de Mendoza, *Congreso Geológico*
619 *Argentino*, pp. 579-592.
- 620 Gulisano, C.A., Gutiérrez Pleimling, A.R., Digregorio, R.E., 1984. Esquema estratigráfico de la
621 secuencia jurásica del oeste de la provincia del Neuquén, *Congreso Geológico Argentino*, pp. 236-
622 259.
- 623 Gulisano, C., Gutiérrez Pleimling, A., 1994. The Jurassic of the Neuquén Basin, a) Neuquén Province-
624 Field Guide. *Asociación Geológica Argentina, Serie E2*, Buenos Aires, Argentina.
- 625 Hodgson, D., Brooks, H.L., Ortiz-Karpf, A., Sychala, Y., Lee, D.R., Jackson, C.A., 2018. Entrainment
626 and abrasion of megaclasts during submarine landsliding and their impact on flow behaviour.
627 *Geological Society, London, Special Publications*, 477, 223-240.
- 628 Hampson, G.J., 2000. Discontinuity Surfaces, Clinoforms, and Facies Architecture in a Wave-
629 Dominated, Shoreface-Shelf Parasequence. *Journal of Sedimentary Research* 70, 325-340.
- 630 Howard J.D., Reineck H.-E., 1981. Depositional facies of high energy beach-to-offshore sequence,
631 comparison with low energy sequence. *APPG Bulletin*, 65, 807-830.
- 632 Howell, J.A., Flint, S.S., 1996. A model for high resolution sequence stratigraphy within extensional
633 basins. *Geological Society, London, Special Publications* 104, 129-137.
- 634 Howell, J.A., Schwarz, E., Spalletti, L.A., Veiga, G.D., 2005. The Neuquén Basin: an overview.
635 *Geological Society, London, Special Publications* 252, 1-14.
- 636 Isla, M.F., Coronel, M., Schwarz, E., Veiga G.D., 2020a. Depositional architecture of a wave-
637 dominated clastic shoreline (Pilmatué Member, Argentina): improving knowledge about the

638 preservation of bar-trough systems. *Marine and Petroleum Geology*. doi:
639 10.1016/j.marpetgeo.2020.104417.

640 Isla, M.F., Schwarz, E., Veiga G.D., 2020b. The record of a non-barred clastic shoreline. *Geology*, 48.
641 doi:10.1130/G46800.1.

642 Johnson, H.D., Baldwin, C.T., 1996. Shallow clastic seas, in: Reading, H.R. (Ed.), *Sedimentary*
643 *Environments: Processes, Facies and Stratigraphy*, 3rd ed. Blackwell, pp. 232–280.

644 Legarreta, L., Uliana, M.A., 1991. Jurassic—Marine Oscillations and Geometry of Back-Arc Basin Fill,
645 Central Argentine Andes, in: Macdonald, D.I.M. (Ed.), *Sedimentation, Tectonics and Eustasy:*
646 *Sedimentation, Tectonics and Eustasy: Sea-Level Changes at Active Margins*. Blackwell Scientific, pp.
647 429-450.

648 Legarreta, L., Uliana, M.A., 1996. The Jurassic succession in west-central Argentina: stratal patterns,
649 sequences and paleogeographic evolution. *Palaeogeography, Palaeoclimatology, Palaeoecology*
650 120, 303-330.

651 Løseth, T.M., Ryseth, A.E., Young, M., 2009. Sedimentology and sequence stratigraphy of the middle
652 Jurassic Tarbert Formation, Oseberg South area (northern North Sea). *Basin Research* 21, 597-619.

653 MacEachern, J.A., Bann, K.L., 2008. The Role of Ichnology in Refining Shallow Marine Facies Models,
654 in: Hampson, G.J., Steel, R.J., Burgess, P.M., Dalrymple, R.W. (Eds.), *Recent Advances in Models of*
655 *Siliciclastic Shallow-Marine Stratigraphy*. SEPM Society for Sedimentary Geology, p. 0.

656 MacEachern, J.A., Pemberton, S.G., 1992. Ichnological Aspects of Cretaceous Shoreface Successions
657 and Shoreface Variability in the Western Interior Seaway of North America, *Applications of*
658 *Ichnology to Petroleum Exploration*, pp. 57-84.

659 MacEachern, J.A., Pemberton, S.G., Bann, K.L., Gingras, M.K., 2007. Departures from the Archetypal
660 Ichnofacies: Effective Recognition of Physico-Chemical Stresses in the Rock Record, in: MacEachern,
661 J.A., Bann, K.L., Gingras, M.K., Pemberton, S.G. (Eds.), *Applied Ichnology*. SEPM Society for
662 *Sedimentary Geology, Short Course Notes* 52, pp. 65-93.

663 MacEachern, J.A., Zaitlin, B.A., Pemberton, S.G., 1999. A sharp-based sandstone of the Viking
664 Formation, Joffre Field, Alberta, Canada; criteria for recognition of transgressively incised shoreface
665 complexes. *Journal of Sedimentary Research* 69, 876-892.

666 Mannie, A.S., Jackson, C.A.-L., Hampson, G.J., 2014. Structural controls on the stratigraphic
667 architecture of net-transgressive shallow-marine strata in a salt-influenced rift basin: Middle-to-
668 Upper Jurassic Egersund Basin, Norwegian North Sea. *Basin Research* 26, 675-700.

669 Mannie, A.S., Jackson, C.A.-L., Hampson, G.J., Fraser, A.J., 2016. Tectonic controls on the spatial
670 distribution and stratigraphic architecture of a net-transgressive shallow-marine synrift succession
671 in a salt-influenced rift basin: Middle to Upper Jurassic, Norwegian Central North Sea. *Journal of the*
672 *Geological Society* 173, 901-915.

673 Morris, J.E., Hampson, G.J., Johnson, H.D., 2006. A sequence stratigraphic model for an intensely
674 bioturbated shallow-marine sandstone: the Bridport Sand Formation, Wessex Basin, UK.
675 *Sedimentology* 53, 1229-1263.

676 Niedoroda, A.W., Swift, D.J.P., Thorne, J.A., 1989. Modeling shelf storm beds: controls of bed
677 thickness and bedding sequence, in: Morton, R.A., Nummedal, D. (Eds.), Shelf sedimentation, shelf
678 sequences and related hydrocarbon accumulation. Proceedings of the 17th annual research
679 conference, Gulf Coast Section. Society of Economic Paleontologists and Mineralogists Foundation,
680 pp. 15-39.

681 Onyenanu, G.I., Jacquemyn, C.E.M.M., Graham, G.H., Hampson, G.J., Fitch, P.J.R., Jackson, M.D.,
682 2018. Geometry, distribution and fill of erosional scours in a heterolithic, distal lower shoreface
683 sandstone reservoir analogue: Grassy Member, Blackhawk Formation, Book Cliffs, Utah, USA.
684 *Sedimentology* 65, 1731-1760.

685 Pemberton, S.G., MacEachern, J.A., Dashtgard, S.E., Bann, K.L., Gingras, M.K., Zonneveld, J.-P., 2012.
686 Shorefaces, in: Knaust, D., Bromley, R.G., (Eds.), Trace Fossils as Indicators of Sedimentary
687 Environments. *Developments in Sedimentology* 64, Elsevier, pp. 563-603.

688 Plint, A.G., 2010. Wave- and storm-dominated shoreline and shallow-marine systems, in: James,
689 N.P., Dalrymple, R.W. (Eds.), *Facies Models 4*. Geological Association of Canada, St. John's, pp. 167–
690 200.

691 Privat, A., Hodgson, D.M., Jackson, C.A.-L., Schwarz, E., Peakall, J., accepted. Evolution from syn-rift
692 carbonates to early post-rift deep-marine intraslope lobes: the role of rift basin physiography on
693 sedimentation patterns. *Sedimentology*.

694 Ravnås, R., Bondevik, K., Helland-Hansen, W., Lømo, L., Ryseth, A., Steel, R.J., 1997. Sedimentation
695 history as an indicator of rift initiation and development: the late Bajocian-Bathonian evolution of
696 the Oseberg-Brage area, northern North Sea. *Norsk Geologisk Tidsskrift* 77, 205-232.

697 Ravnås, R., Steel, R.J., 1998. Architecture of Marine Rift-Basin Successions. *AAPG Bulletin* 82, 110-
698 146.

699 Reading, H.G., Collinson, J.D., 1996. Clastic coasts, in: Reading, H.G. (Ed.), *Sedimentary*
700 *Environments: Processes, Facies and Stratigraphy*. 3rd ed. Blackwell Science, pp. 154-231.

701 Reineck, H.-E., 1977. Natural indicators of energy level in Recent sediments: the application of
702 ichnology to a coastal engineering problem, in: Crimes, T.P., Harper, J.C. (Eds.), *Trace Fossils* 2, pp.
703 265–272.

704 Riccardi, A.C., 2008. El Jurásico de la Argentina y sus amonites. *Revista de la Asociación Geológica*
705 *Argentina* 63, 625-643.

706 Sagripanti, L., Folguera, A., Giménez, M., Vera, E.R., Fabiano, J., Molnar, N., Fennell, L., Ramos, V.A.,
707 2014. Geometry of Middle to Late Triassic extensional deformation pattern in the Cordillera del
708 Viento (Southern Central Andes): A combined field and geophysical study. *Journal of Iberian Geology*
709 40, 349-366.

710 Schwarz, E., Álvarez-Trentini, G., Valenzuela, M.E., 2013. Ciclos mixtos carbonáticos/silicoclásticos
711 en el Miembro Superior de la Formación Mulichinco (yacimiento Cañadón Amarillo, Cuenca
712 Neuquina central): Implicancias secuenciales y para caracterización de reservorios. *Latin American*
713 *Journal of Sedimentology and Basin Analysis* 20, 21-49.

- 714 Schwarz, E., Veiga, G.D., Álvarez Trentini, G., Spalletti, L.A., 2016. Climatically versus Eustatically
715 Controlled, Sediment-Supply-Driven Cycles: Carbonate-Siliciclastic, High-Frequency Sequences in
716 the Valanginian of the Neuquén Basin (Argentina). *Journal of Sedimentary Research* 86, 312-335.
- 717 Schwarz, E., Veiga, G.D., Álvarez Trentini, G., Isla, M.F., Spalletti, L.A., 2018. Expanding the spectrum
718 of shallow-marine, mixed carbonate–siliciclastic systems: Processes, facies distribution and
719 depositional controls of a siliciclastic-dominated example. *Sedimentology* 65, 1558-1589.
- 720 Snedden, J.W., Nummedal, D., 1991. Origin and geometry of storm-deposited sand beds in modern
721 sediments of the Texas Continental Shelf, in: Swift, D.J.P., Oertel, G.F., Tillman, R.W., Thorne, J.A.
722 (Eds.), *Shelf Sand and Sandstone Bodies*. International Association of Sedimentologists Special
723 Publication, 14, pp. 283-308.
- 724 Spalletti, L.A., Parent, H., Veiga, G.D., Schwarz, E., 2012. Amonites y Bioestratigrafía del Grupo Cuyo
725 en la Sierra de Reyes (Cuenca Neuquina central, Argentina) y su significado secuencial. *Andean
726 Geology* 39, 464-481.
- 727 Taylor, A.M., Goldring, R., 1993. Description and analysis of bioturbation and ichnofabric. *Journal of
728 the Geological Society* 150, 141-148.
- 729 Veiga, G.D., Schwarz, E., Spalletti, L.A., 2011. Análisis estratigráfico de la Formación Lotena
730 (Calloviano superior-Oxfordiano inferior) en la Cuenca Neuquina Central, República Argentina:
731 Integración de información de afloramientos y subsuelo. *Andean Geology* 38, 171-197.
- 732 Veiga, G.D., Schwarz, E., Spalletti, L.A., Massaferro, J.L., 2013. Anatomy and sequence architecture
733 of the early post-rift in the Neuquén Basin (Argentina): a response to physiography and relative sea-
734 level changes. *Journal of Sedimentary Research* 83, 746-765.
- 735 Vergani, G.D., Tankard, A.J., Belotti, H.J., Welsink, H.J., 1995. Tectonic evolution and paleogeography
736 of the Neuquén Basin, Argentina, in: Tankard, A.J., Suárez Soruco, R., Welsink, H.J. (Eds.), *Petroleum
737 Basins of South America*. AAPG Memoirs, 62, pp. 383-402.
- 738 Walker, R.G., Plint, A.G., 1992. Wave- and storm-dominated shallow marine systems, in: Walker
739 R.G., James, N.P. (Eds.), *Facies Models: Response to sea level change*. Geological Association of
740 Canada, pp. 219-238.
- 741 Walsh, J.P., Corbett, D.R., Alexander, C.R., 2018. Source-to-sink sedimentation: insights from
742 modern continental-margin system studies. 20th International Sedimentological Congress, 13-17th
743 August 2018, Québec City, Canada. Poster presentation.
- 744 Wetzel, A. and Uchman, A., 1998. Biogenic sedimentary structures in mudstones – an overview. In:
745 Schieber, J., Zimmerle, W., Sethi, P. (Eds.), *Shales and Mudstones*. Schweizerbart, pp. 351–369.
- 746 Wheatcroft, R.A., 1990. Preservation potential of sedimentary event layers. *Geology* 18, 843-845.

747

748 **FIGURES AND FIGURE CAPTIONS**

749 **Fig 1. A.** Map of the Neuquén Basin with approximate location (red square) of the study area (Fig.
750 2). CM: Chacay Melehue area; PL: Picún Leufú area; PM: Potimalal area; SR: Sierra de Reyes (Study
751 area) **B.** Paleogeographic reconstruction of the Neuquén Basin during the Jurassic – Early-
752 Cretaceous. The onset of subduction on the western margin of Gondwana and the early
753 development of the Andean arc led to development of a large triangular-shape epicontinental basin,
754 partially connected to the proto-Pacific Ocean through a volcanic arc. Modified after Howell et al.
755 (2005).

756 **Fig. 2. A.** Cross-section (integrating outcrop and well data) showing the stratigraphic setting and
757 overall depositional architecture of the early post-rift succession (Bardas Blancas, Los Molles and
758 Lajas formations) in central Neuquén Basin, as well as the older Remoredo Formation (syn-rift
759 volcanoclastic deposits) and Choiyoi Group (basement) units. Inset shows detailed map of the cross-
760 section. Modified from Veiga et al. (2013). **B.** Chronostratigraphic chart for the study area, showing
761 the temporal distribution of the Cuyo Group succession. Asterisks (Levels 1 to 4) show the location
762 of ammonite levels described by Spalletti et al. (2012). The studied Bardas Blancas Formation
763 (Toarcian-Bathonian) would represent a time interval ranging from 7 Myr to 10 Myr.

764 **Fig. 3. A.** Geologic map of the Sierra de Reyes region, showing the different locations studied by
765 Veiga et al. (2013) (black stars) and this study (white stars). **B.** Satellite image of the study area, in
766 the eastern flank of the Sierra de Reyes anticline, showing the location of the sections studied in
767 the Cuyo Group.

768 **Fig. 4. A.** Field panoramas of Agua del Campo (**A**) and Agua de Heredia (**B**), showing the location of
769 main stratigraphic units, and their bounding surfaces. **C.** Simplified stratigraphic section showing the
770 overall aggradational-to-retrogradational stacking of the Bardas Blancas Formation, and its vertical
771 relationships with the underlying and overlying lithostratigraphic units. Parasequence sets (PSS's)
772 after Veiga et al. (2013).

773 **Fig. 5.** Outcrop examples of the different facies associations defined in this study. **A.** Cross-bedded,
774 organic-rich and poorly-sorted pebbly to medium-grained sandstones (FA1 - Delta Front).
775 Parasequence Set I, Agua de Heredia. **B.** Amalgamated, trough cross-bedded, well-sorted fine-
776 grained sandstones (FA2 – Upper shoreface). Parasequence Set I, Agua de Heredia. **C.** Tabular to
777 slightly undulate, medium-bedded fine-grained sandstones, with hummocky cross-stratification
778 (HCS) (FA3 - Lower shoreface). Parasequence Set II, Agua del Campo. **D.** Moderate to highly
779 bioturbated sandstones and muddy sandstones, with local preservation of HCS (FA4 - Offshore
780 transition). Parasequence Set II, Agua del Campo. **E.** Highly bioturbated sandy and silty mudstones,
781 with subordinate muddy sandstones (FA5 - Proximal offshore). Parasequence Set II, Agua de
782 Heredia. **F.** Massive to crudely laminated gray mudstones with occasional diagenetic nodule-rich
783 horizons (FA6 - Distal offshore). Parasequence Set II, Agua de Heredia. See Table 1 for more details
784 about their main attributes, and Figs. 2 and 4 for location in stratigraphy.

785 **Fig. 6.** Selected examples of trace fossils found in offshore transition (FA4) and proximal offshore
786 (FA5) facies associations.

787 **Fig. 7.** General depositional model of the Bardas Blancas Formation in the study area, showing the
788 distribution of different facies associations (FA's) and their associated depositional environments.
789 Note the influence of inherited and under-filled rift topography in the stratigraphic architecture of

790 early post-rift deposits. Also note that the fluvial entry point and deltaic system within the study
791 area would apply for the early stages of evolution. Not to scale.

792 **Fig. 8.** Architecture, bedding and bioturbation of the study interval at different scales. **A.** Detailed
793 stratigraphic section with the lithological, sedimentary and bioturbation trends of a 10's of m-thick,
794 shallowing-up succession (parasequence), made by several m-scale bedsets, and bounded by
795 regional-scale flooding surfaces. Parasequence Set II, Agua de Heredia. See Figs. 2 and 4 for location
796 in stratigraphy. **B.** Highly bioturbated, dm-scale muddy sandstones and sandy mudstones in offshore
797 transition deposits (FA5). Parasequence Set III, Agua del Ñaco. **C.** Bioturbated offshore transition
798 deposits (FA5), stacked in m-scale, well-defined bedsets. Parasequence Set III, Agua de Ñaco. **D.**
799 General view of several m-scale bedsets, showing the homogeneous and tabular nature of the
800 studied deposits. Parasequence Set II, Agua de Heredia. See stratigraphic position in A.

801 **Fig. 9.** Two examples of preserved HCS in storm beds. **A.** General view of the gradual vertical
802 transition from proximal offshore (FA5) to offshore transition deposits (FA4). **B.** Example of partially
803 preserved HCS in dominantly highly bioturbated proximal offshore deposits (FA5). Parasequence Set
804 II, Agua de Heredia. **C.** Detailed view of the contact between the fully bioturbated (*Chondrites*
805 ichnofabric) upper part and the non-bioturbated lower part (preserving the original sedimentary
806 structures) of the same event bed. Parasequence Set II, Agua de Heredia. **D.** Outcrop view of
807 offshore transition deposits (FA4). **E.** Example of preserved HCS in a partially mixed event bed,
808 overlain and underlain by highly bioturbated muddy sandstones and sandy mudstones (offshore
809 transition, FA4). Parasequence Set III, Agua del Campo Sur.

810 **Fig. 10.** GR well logs and core examples of highly bioturbated, storm-dominated shallow-marine
811 successions comparable to the studied deposits. **A.** Upper Jurassic Farsund Formation, interpreted
812 as the equivalent offshore transition deposits of the bioturbated, sand-rich Ula Formation in the
813 Norwegian Central Graben. **B.** Heather and Intra-Heather Sandstone Formation, the offshore
814 transition deposits overlying the transgressive shallow-marine sandstones of the Tarbert Formation,
815 in Northern Viking Graben/Western Horda Platform. **C.** Heather Formation, also the equivalent
816 offshore transition deposits of the highly bioturbated, Fulmar Formation, in the UK Central Graben.
817 **D.** Lower-Middle Jurassic Bardas Blancas Formation, Neuquén Basin (this study).

818 **Fig. 11.** Structural setting, overall stratigraphic architecture and stacking pattern of the different
819 highly bioturbated, storm-dominated shallow-marine successions shown in Figure 10, and the
820 Bardas Blancas Formation.

821

822 **Table 1.** Facies association classification, description and interpretation of the main processes and
823 environments of deposition. Trace fossil content is listed in relative order of abundance. FWWB:
824 Fair-weather wave-base; SWWB: Storm-weather wave-base.

825 **Table 2.** Main characteristics of the thick, intensely bioturbated successions discussed in this
826 contribution.

827

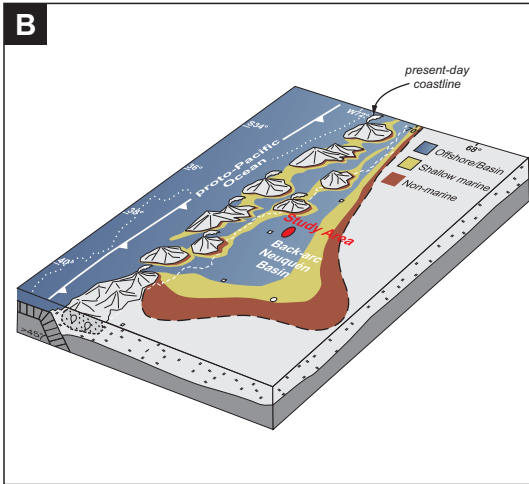
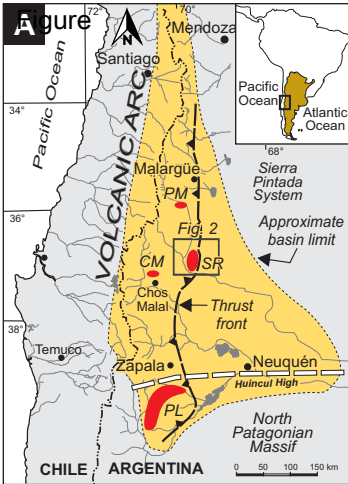
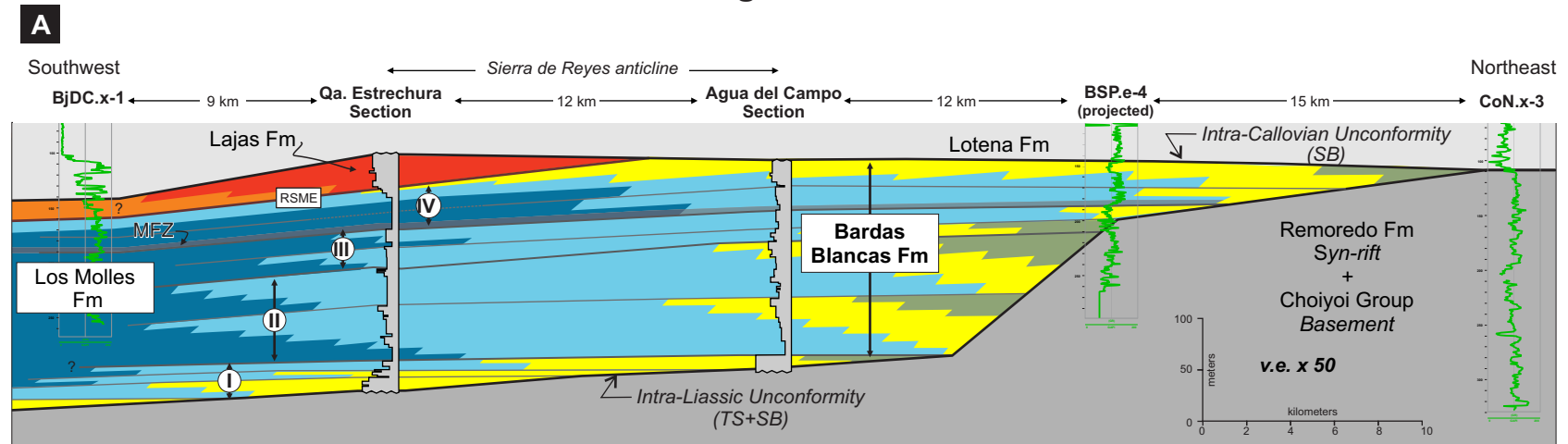


Figure 2

Figure 2



- Coastal-plain deposits (inferred)
- Shoreface deposits
- Offshore-transition and upper offshore deposits
- Lower offshore deposits
- Deltaic deposits (proximal delta front to ?distal delta front)
- Flooding surface bounding PS
- Flooding surface bounding PS set
- II Parasequence set I to IV
- MFZ Maximum flooding zone
- RSME Regressive surface of marine erosion
- TS Transgressive surface
- SB Sequence Boundary
- ~174 Selected stage boundary (Myr)
- L.J. Lower Jurassic

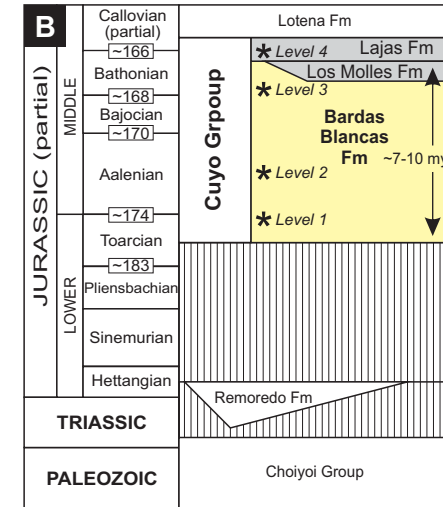
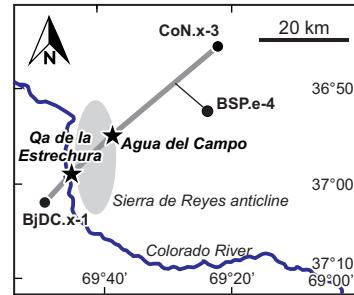


Figure 3

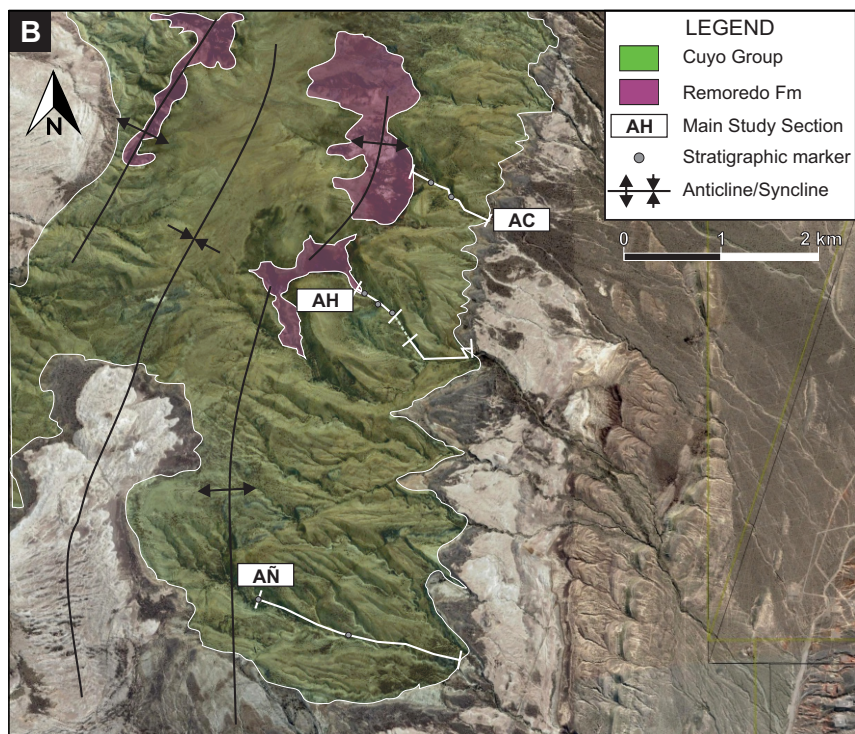
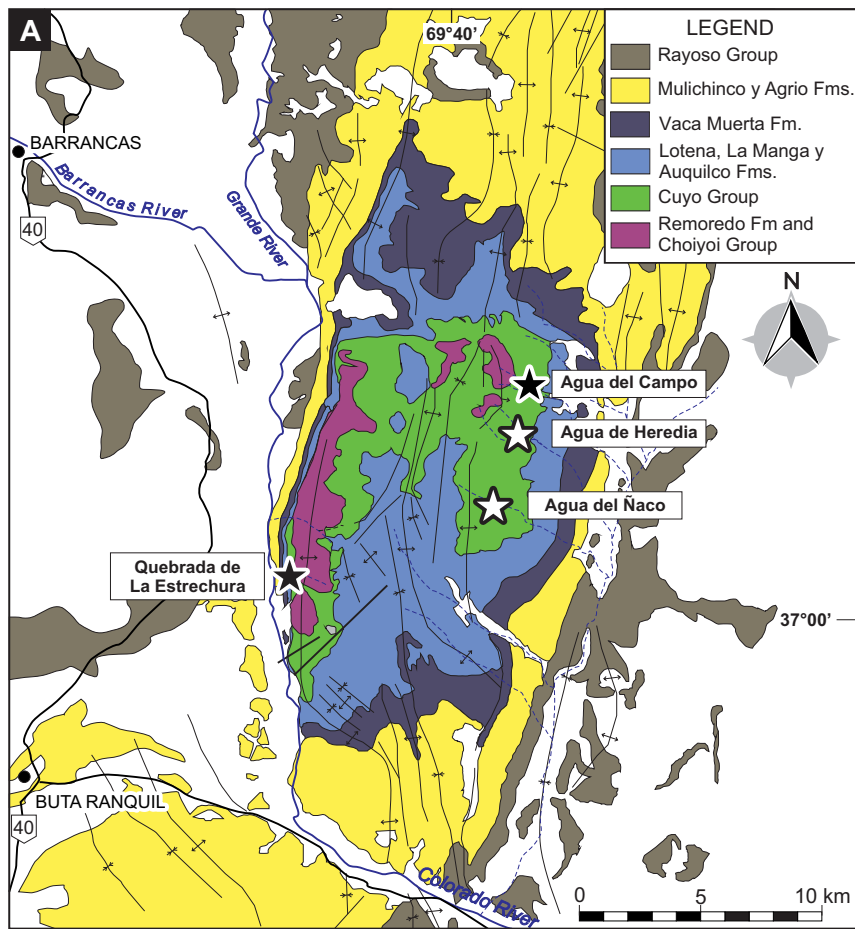


Figure 4

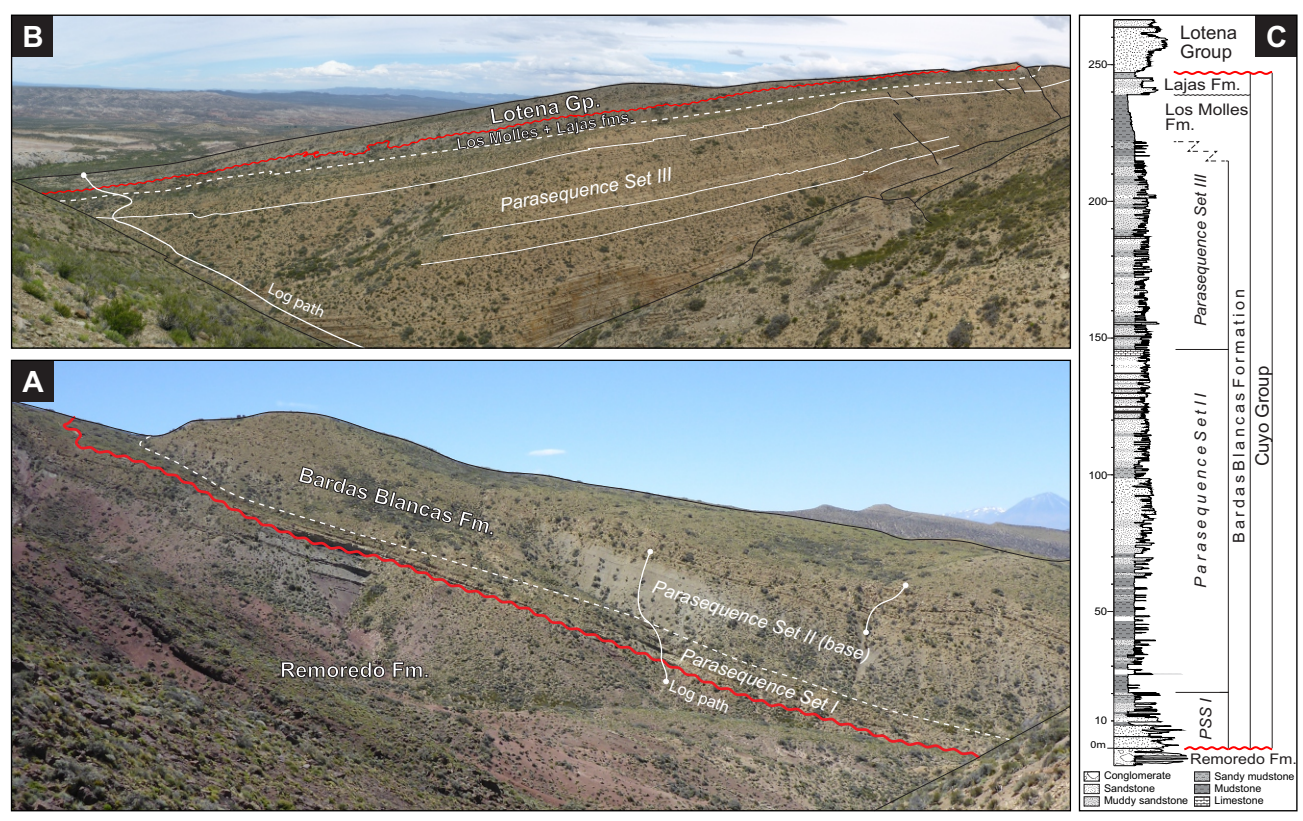


Figure 5



Figure 06

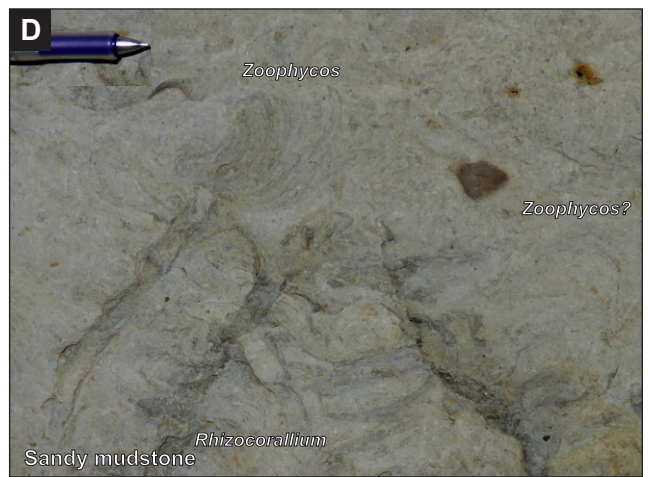
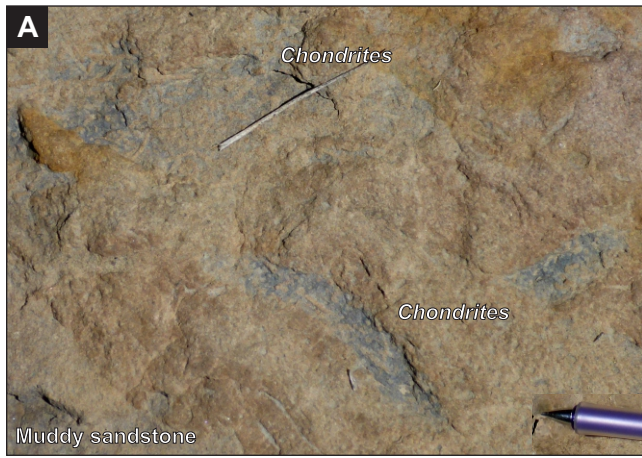


Figure 7

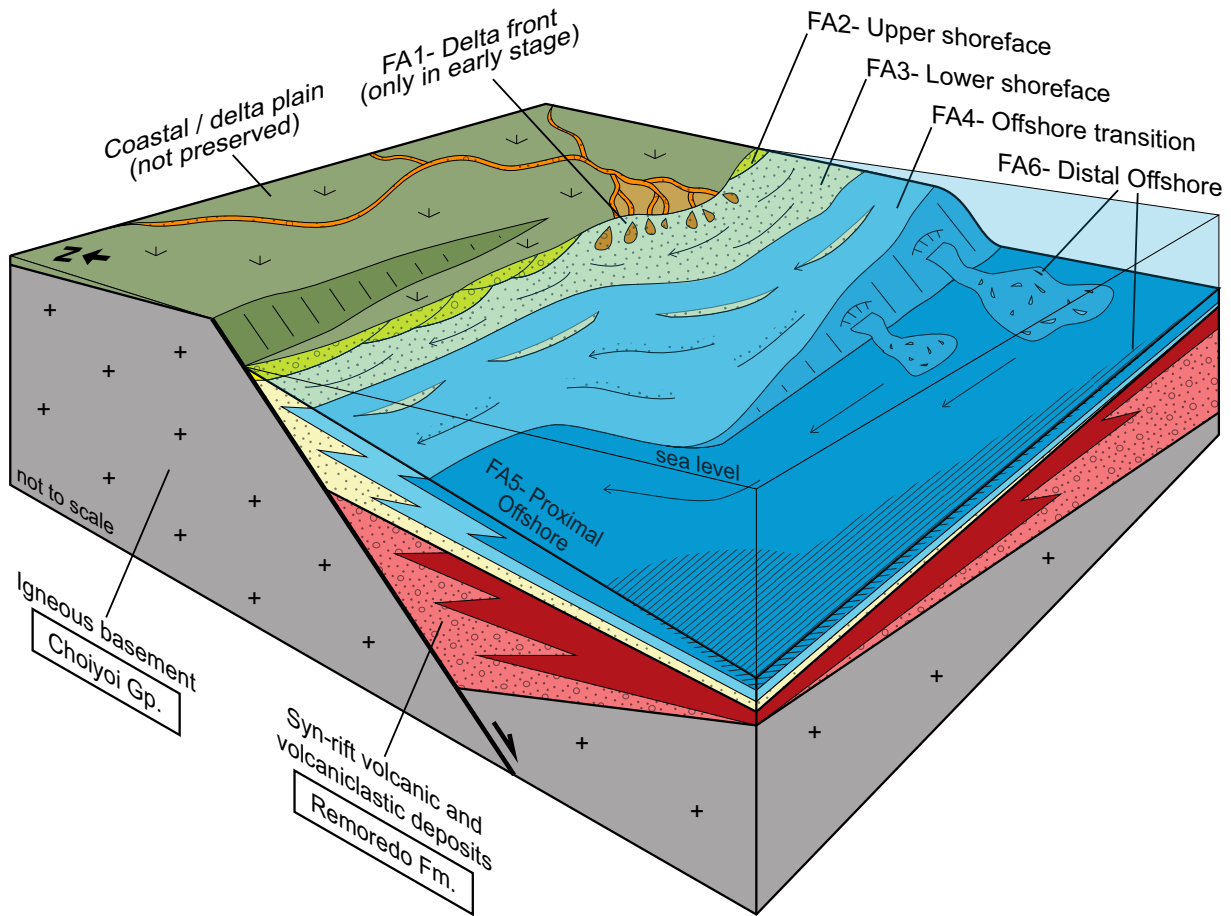


Figure 8

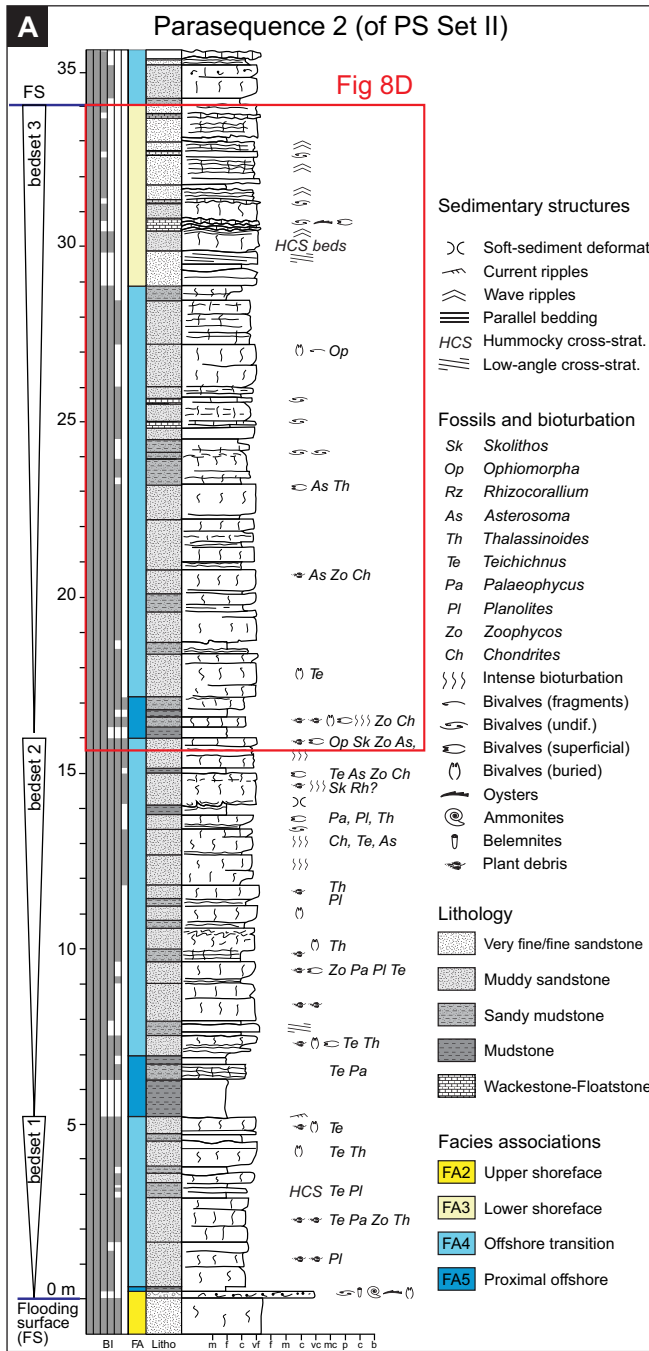


Figure 9

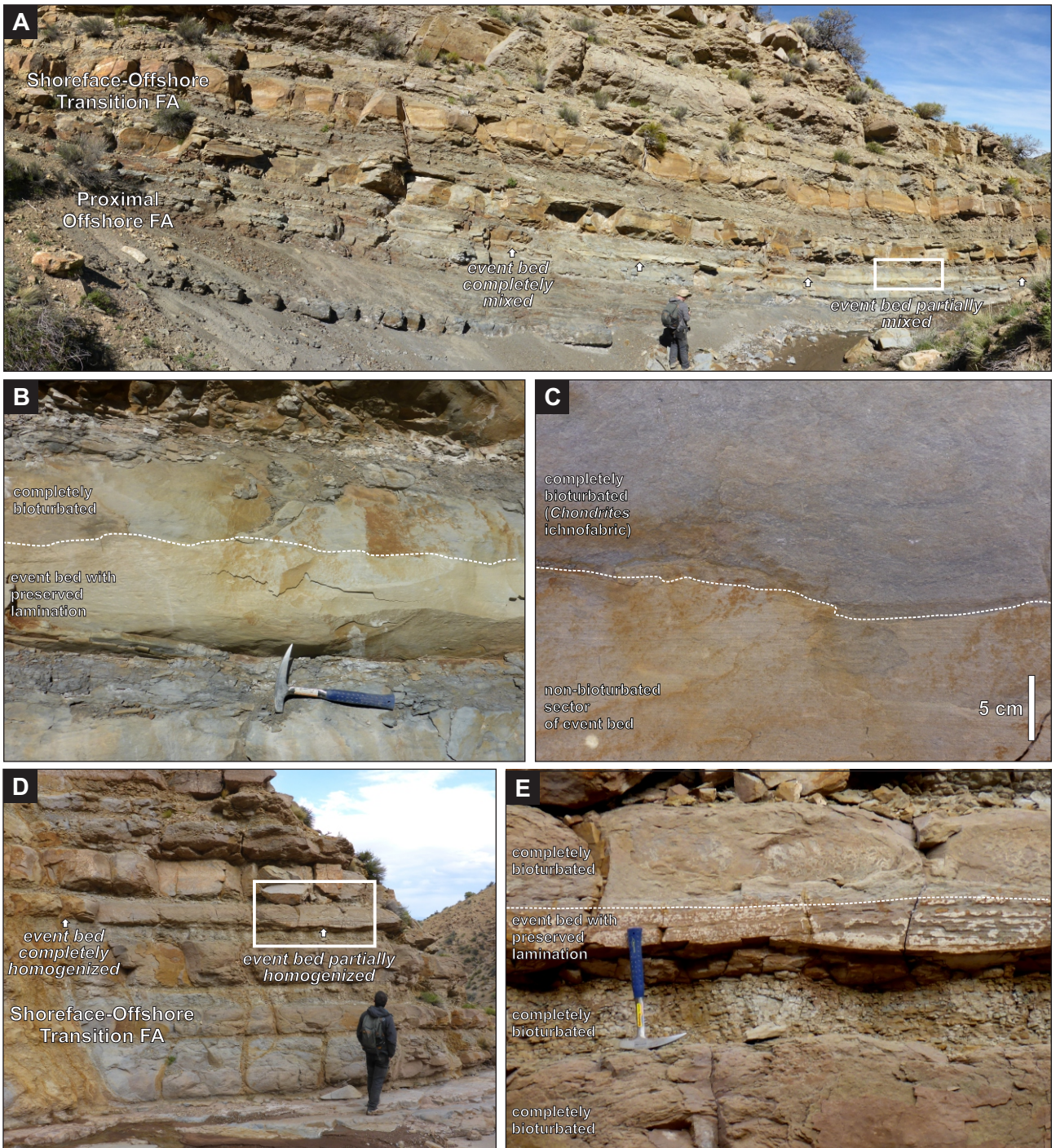
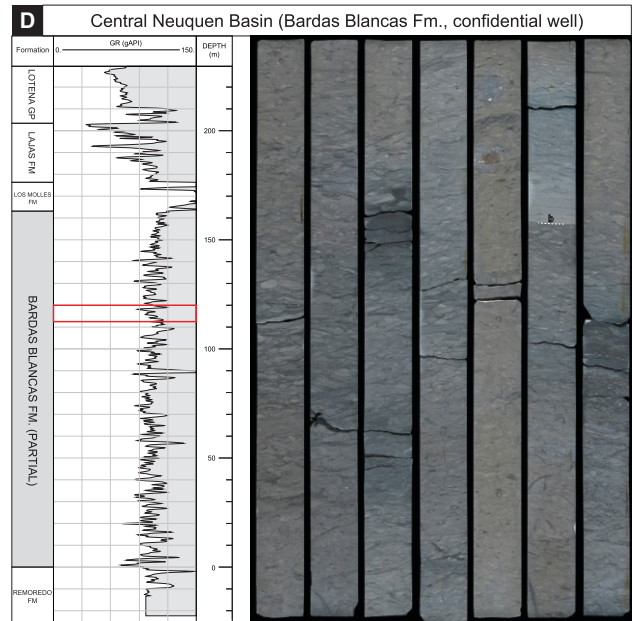
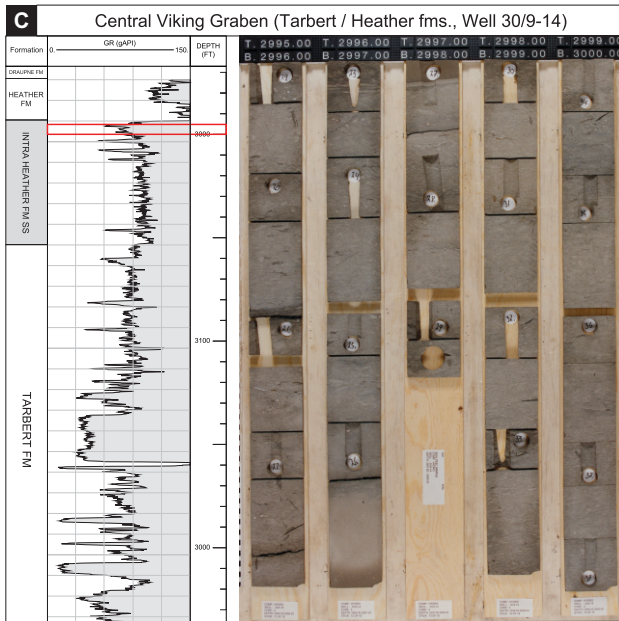
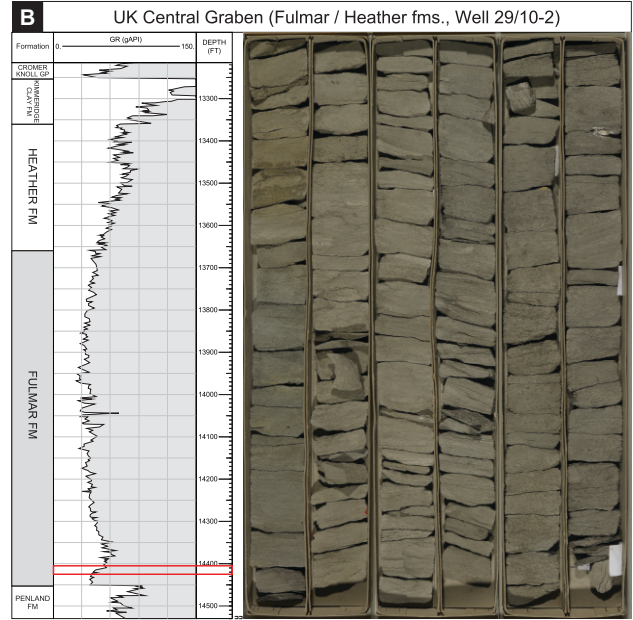
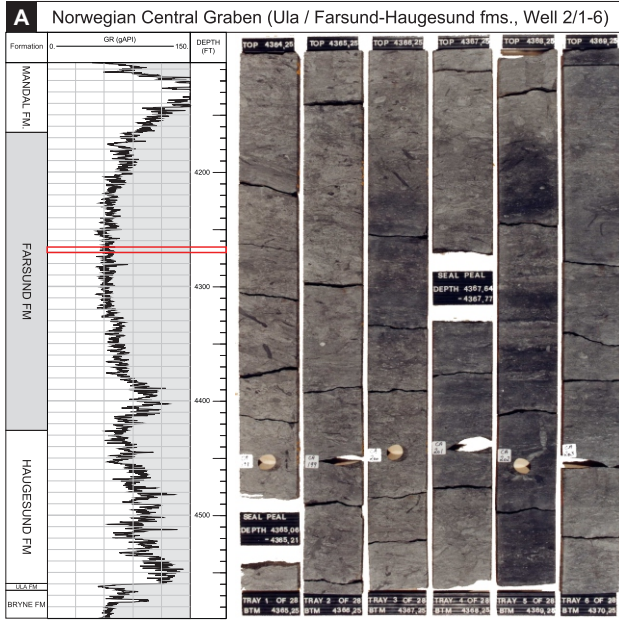
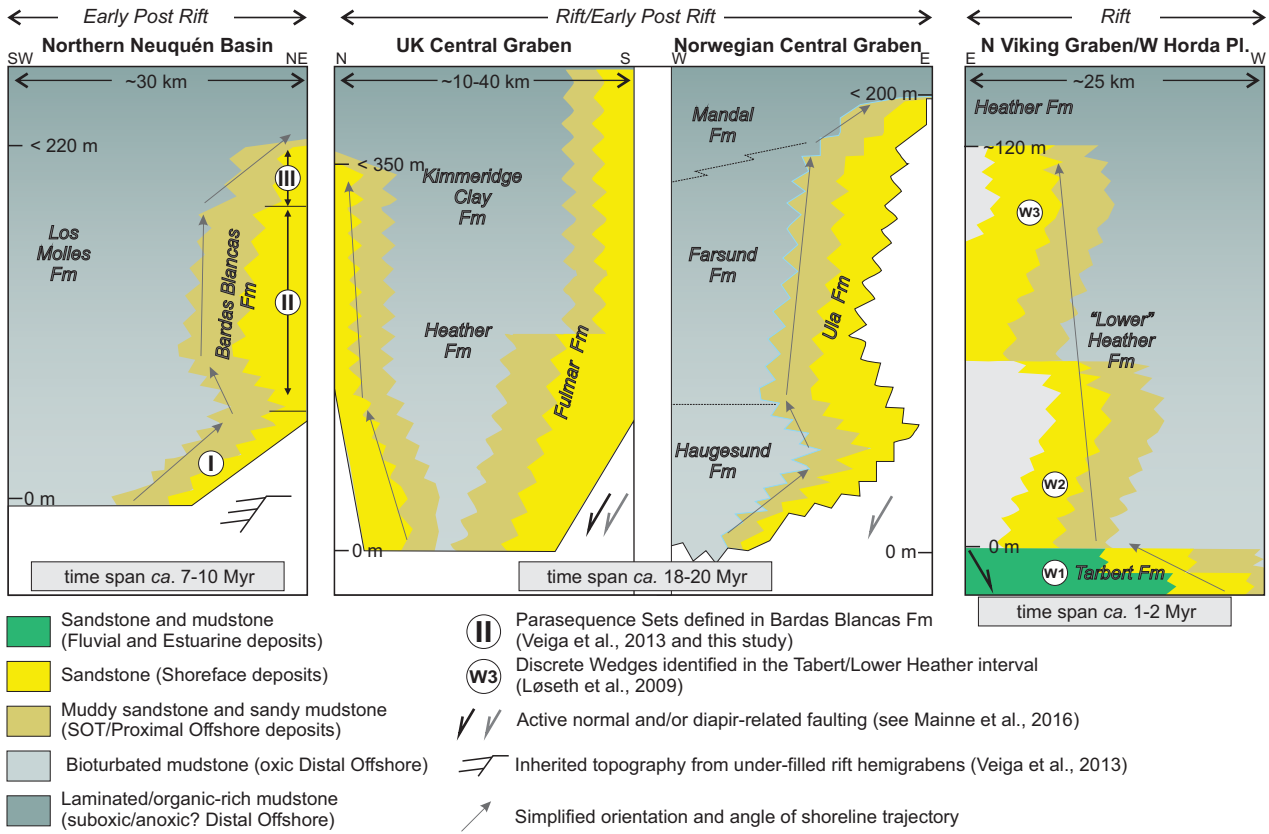


Figure 10



cored interval shown

Figure 11

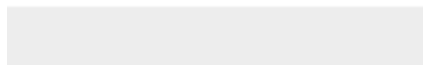




[Click here to access/download](#)

Table

Schwarz et al_Table 1_0341.docx

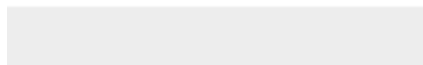




Click here to access/download

Table

Schwarz et al_Table 2_0341.docx



Conflict of interests with following researchers

Carlos Zavala

Pablo Pazos